© 2017. Published by The Company of Biologists Ltd | Journal of Cell Science (2017) 130, 3419 doi:10.1242/jcs.210682

PUBLISHER'S NOTE

Publisher's Note: Chromosomal breaks during mitotic catastrophe trigger γH2AX–ATM–p53-mediated apoptosis. Gabriela Imreh, Helin Vakifahmetoglu Norberg, Stefan Imreh, Boris Zhivotovsky. J. Cell Sci. doi: 10.1242/jcs.081612

Michael Way
Editor-in-Chief, Journal of Cell Science (jcs@biologists.com)

This Publisher's Note updates and replaces the Expression of Concern (J. Cell Sci. 2017 **130**, 1979; doi: 10.1242/jcs.205559) relating to the article 'Chromosomal breaks during mitotic catastrophe trigger γH2AX–ATM–p53-mediated apoptosis' by Gabriela Imreh, Helin Vakifahmetoglu Norberg, Stefan Imreh and Boris Zhivotovsky. J. Cell Sci. 2011 **124**, 2951-2963 (doi: 10.1242/jcs.081612).

Concerns were raised regarding some of the data in Fig. 1A of the above-named paper. An investigation carried out by Karolinska Institutet concluded that no wrongdoing had occurred, and that no further action was required. An in-house review of the original data by Journal of Cell Science reached a similar conclusion.

Journal of Cell Science is publishing this Note to alert readers that the concerns raised about this paper have been resolved.

This course of action follows the advice set out by COPE (Committee on Publication Ethics), of which Journal of Cell Science is a member.

© 2017. Published by The Company of Biologists Ltd | Journal of Cell Science (2017) 130, 1979 doi:10.1242/jcs.205559

PUBLISHER'S NOTE

Expression of Concern: Chromosomal breaks during mitotic catastrophe trigger γH2AX–ATM–p53-mediated apoptosis. Gabriela Imreh, Helin Vakifahmetoglu Norberg, Stefan Imreh, Boris Zhivotovsky. J. Cell Sci. doi: 10.1242/jcs.081612

Michael Way
Editor-in-Chief, Journal of Cell Science (jcs@biologists.com)

This Expression of Concern relates to the article 'Chromosomal breaks during mitotic catastrophe trigger γH2AX–ATM–p53-mediated apoptosis' by Gabriela Imreh, Helin Vakifahmetoglu Norberg, Stefan Imreh and Boris Zhivotovsky. *J. Cell Sci.* (2011) **124**, 2951-2963 (doi: 10.1242/jcs.081612).

Concerns have been raised regarding some of the data in Fig. 1A of the above-named paper. Journal of Cell Science is publishing this note to make readers aware of this issue, and we will provide further information once the issue has been resolved.

This course of action follows the advice set out by COPE (Committee on Publication Ethics), of which Journal of Cell Science is a member.

© 2016. Published by The Company of Biologists Ltd | Journal of Cell Science (2016) 129, 1950 doi:10.1242/jcs.190132

CORRECTION

Chromosomal breaks during mitotic catastrophe trigger γH2AX–ATM–p53-mediated apoptosis

Gabriela Imreh, Helin Vakifahmetoglu Norberg, Stefan Imreh and Boris Zhivotovsky

There was an error published in *J. Cell Sci.* **124**, 2951–2963.

In Fig. 4C, the blot representing pATM was inadvertently duplicated as representing G3PDH. The G3PDH western blot has been replaced with the correct image in the figure shown below. There are no changes to the figure legend, which is accurate. This error does not affect the conclusions of the study.

The authors apologise to the readers for any confusion that this error might have caused.

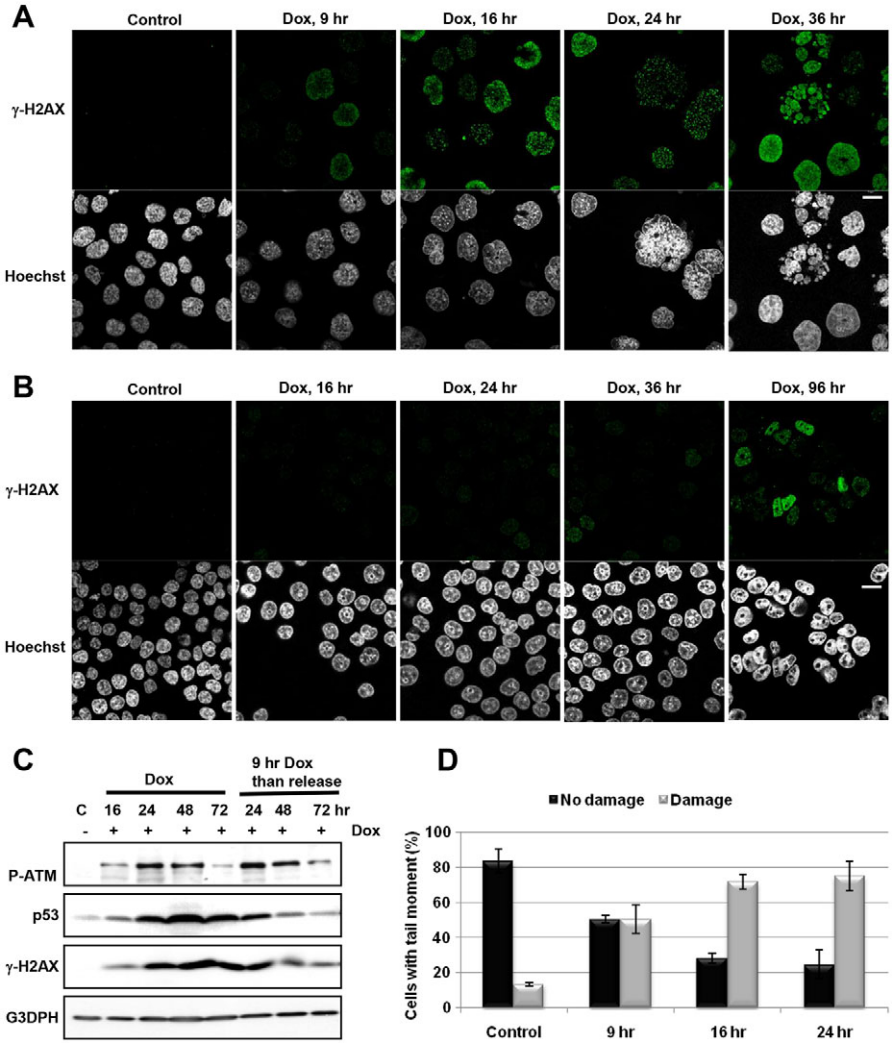

Fig. 4. Increased γH2AX level during MC leads to cell death. Untreated or doxorubicin (600 nM)-treated 14-3-3σ-knockout HCT116 cells were cultured and harvested at indicated time points and analysed by western blot (50 µg), comet assay and immunostaining using antibodies directed against γH2AX (green). Blots were reprobed for G3PDH to confirm an equal loading of the samples. The co-staining of nuclei was performed using Hoechst 33342 (white). (A,B) Representative confocal images showing nuclear morphology and γH2AX staining in 14-3-3σ-knockout HCT116 (A) or wild-type HCT116 (B) cells after treatment for indicated time. (C) 14-3-3σ-knockout HCT116 cells were treated for 9 hours with doxorubicin after which the culture medium was replaced and cells were grown for an additional 24, 48 and 72 hours. Immunoblots of p53, phosphorylated ATM and γH2AX are shown. (D) Doxorubicin-induced DNA damage measured by alkaline comet assay. Cells were analysed by fluorescence microscopy and scored according to tail moment. Error bars represent the mean of three independent experiments±s.e.m. Scale bar: 20 µm.

Journal of Cell Science

Chromosomal breaks during mitotic catastrophe trigger γH2AX–ATM–p53-mediated apoptosis

Gabriela Imreh[1,*], Helin Vakifahmetoglu Norberg[2,*], Stefan Imreh[3] and Boris Zhivotovsky[1,‡]

[1]Division of Toxicology, Institute of Environmental Medicine, Karolinska Institutet, SE-171 77 Stockholm, Sweden
[2]Developmental Biology, Wenner-Gren Institute, Stockholm, University, SE-106 91 Stockholm, Sweden
[3]Department of Microbiology, Tumor and Cell Biology, Karolinska Institutet, Stockholm SE-171 77, Sweden

*These authors contributed equally to this work
‡Author for correspondence (Boris.Zhivotovsky@ki.se)

Accepted 3 May 2011
Journal of Cell Science 124, 2951–2963

doi: 10.1242/jcs.081612

Summary

Although the cause and outcome of mitotic catastrophe (MC) has been thoroughly investigated, precisely how the ensuing lethality is regulated during or following this process and what signals are involved remain unknown. Moreover, the mechanism of the decision of cell death modalities following MC is still not well characterised. We demonstrate here a crucial role of the γH2AX–ATM–p53 pathway in the regulation of the apoptotic outcome of MC resulting from cells entering mitosis with damaged DNA. In addition to p53 deficiency, the depletion of ATM (ataxia telangiectasia mutated), but not ATR (ataxia telangiectasia and Rad3-related protein), protected against apoptosis and shifted cell death towards necrosis. Activation of this pathway is triggered by the augmented chromosomal damage acquired during anaphase in doxorubicin-treated cells lacking 14-3-3σ (also known as epithelial cell marker protein-1 or stratifin). Moreover, cells that enter mitosis with damaged DNA encounter segregation problems because of their abnormal chromosomes, leading to defects in mitotic exit, and they therefore accumulate in G1 phase. These multi- or micronucleated cells are prevented from cycling again in a p53- and p21-dependent manner, and subsequently die. Because increased chromosomal damage resulting in extensive H2AX phosphorylation appears to be a direct cause of catastrophic mitosis, our results describe a mechanism that involves generation of additional DNA damage during MC to eliminate chromosomally unstable cells.

Key words: Apoptosis, Cell death, Checkpoint, Genomic instability, Mitotic catastrophe

Introduction

To maintain genome integrity, cells respond to DNA damage by either a delay in cell cycle progression, allowing time for proper DNA repair, or the elimination of cells carrying irreparable damage. Checkpoints that monitor the cell cycle are capable of inducing arrest at multiple positions, including G1–S transition, S-phase progression and G2–M transition, as well as progression through mitosis. When checkpoints are compromised, cells can enter mitosis prematurely, before the completion of DNA repair, and initiate mitotic catastrophe (MC) (Roninson et al., 2001). The latter is a process occurring either during or shortly after a dysregulated or failed mitosis, and can be accompanied by morphological alterations, including micronucleation (which often results from chromosomes and/or chromosome fragments that have not been distributed evenly between daughter nuclei) and multinucleation (the presence of two or more nuclei with similar or heterogeneous sizes, deriving from a deficient separation during cytokinesis). Tumour cells forced to undergo MC have also been shown to enter an endocyclic process, in which they uncouple DNA replication from the S-phase of the cell cycle and form endopolyploid mononucleated giant cells (Erenpreisa et al., 2005; Waldman et al., 1996; Yu, 1964). The stage of mitosis during which cells start to undergo MC seems to be important for the decision to form various morphological abnormalities specific to MC. Owing to these abnormalities in mitosis, most of the cells undergoing MC eventually die. We have previously characterised both the morphological and biochemical hallmarks of MC and revealed that death-associated MC is not a separate mode of cell death, but rather a process ('pre-stage') preceding cell death, which occurs via necrosis or apoptosis, depending on the molecular profile of the cell (Vakifahmetoglu et al., 2008).

Several DNA-damaging or microtubule-destabilising agents, including antitumor drugs or ionising radiation (Gewirtz, 1999), induce MC, but precisely how the ensuring lethality is regulated and the molecular details of its mechanism have yet to be clarified. Moreover, although MC can lead to apoptosis or necrosis, how and when the decision of the mode of cell death is made and triggered is not known. Studies aiming to elucidate the process of MC in molecular terms have mostly been based on experiments performed on HCT116 human colon carcinoma treated with doxorubicin (Castedo et al., 2004a; Chan et al., 1999). In these studies, the inhibition of checkpoint kinase 2 (Chk2) or the absence of the cell cycle regulator 14-3-3σ was found to facilitate the translocation of the cyclin-dependent kinase 1 (CDK1)–cyclin-B complex to the nucleus, thereby preventing G2 arrest and triggering MC because of entry into mitosis with unrepaired DNA. This premature mitosis is thought to lead to a p53-independent arrest during the metaphase–anaphase transition. If triggered from mitotic arrest, apoptosis has also been suggested to occur independently from p53, but to involve the activation of caspase-2 (Castedo et al., 2004b).

Because several groups have reported that the activation of caspase-2 is dependent on p53, it is likely that apoptosis-induced mitotic arrest would also be p53 dependent (Tinel and Tschopp, 2004; Vakifahmetoglu et al., 2006). Recently, it has been shown that p73 might substitute for p53 in regulating mitotic death (Toh et al., 2010).

We have previously demonstrated that p53 has a critical role in triggering apoptosis following MC induced by DNA damage. Although the presence of functional p53 triggers an apoptotic response in ovarian carcinoma, its absence leads to MC followed by necrosis-like lysis (Vakifahmetoglu et al., 2008). However, although functional p53 is present in 14-3-3σ-knockout HCT116 cells, treatment with doxorubicin drives these cells to undergo MC. The activation of p53 seems to occur following the morphological changes characteristic of MC, and mediates a p53-dependent pathway in which p53 target genes trigger an apoptotic signal, including caspase-2 activation (Vakifahmetoglu et al., 2008). This indicates that although a functional p53 is present in 14-3-3σ-knockout HCT116 cells, the p53-dependent apoptotic program is delayed because of a primary mitotic arrest. Thus, p53 seems to be an important regulator of apoptosis subsequent to MC (Eom et al., 2005; Huang et al., 2005). Nevertheless, the exact molecular mechanism of how p53 is activated during or after MC remains to be elucidated (Loffler et al., 2006; Woods et al., 1995). Hence, the aim of this study was to investigate the molecular link between DNA-damage-induced MC and the subsequent triggering of p53-dependent apoptosis. Here, we demonstrate the essential role of the phosphorylated H2AX (γH2AX)–ataxia-telangiectasia-mutated (ATM)–p53 pathway in the regulation of the apoptotic outcome of MC. In addition to p53 deficiency, the depletion of ATM, but not ATM and Rad3-related protein (ATR), protected against apoptosis and shifted cell death towards necrosis. HCT116 14-3-3σ-knockout cells undergoing MC displayed augmented γH2AX as they entered premature mitosis. This amplified γH2AX foci formation was directly caused by additional double-strand breaks (DSBs), generated during anaphase, that were distinct from those initially caused by the DNA-damaging agent doxorubicin. As increased chromosomal damage seems to be a direct result of MC, our data suggest a mechanism for the generation of a DNA-damage response by the γH2AX–ATM–p53 pathway for the elimination of MC cells.

Results

p53 is required for the apoptotic response following MC

The treatment of 14-3-3σ-knockout HCT116 cells with 600 nM doxorubicin led to an accumulation of cells displaying morphological changes characteristic of MC at 16–24 hours, followed by the appearance of apoptosis-related features (such as the formation of apoptotic bodies and condensed chromatin) at 36–48 hours (Fig. 1A, supplementary material Movies 1–3). This late apoptotic response was accompanied by p53 accumulation, as documented by immunoblotting (Fig. 1B) and, in line with our previous observations, the processing of caspase-2 (Fig. 1B). To elucidate the role of p53 accumulation subsequent to MC, the level of p53 protein was suppressed by siRNA in 14-3-3σ-knockout HCT116 cells (Fig. 1B), and changes in the nuclear morphology following doxorubicin treatment were investigated. Silencing of *TP53* did not influence the development of MC because multinucleated cells were still accumulated in a time-dependent manner upon treatment with doxorubicin (Fig. 1A and supplementary material Fig. S1A). However, in contrast to control cells, most of the p53-deficient 14-3-3σ-knockout HCT116 cells collapsed, lysed and detached from the culture plate starting at 48 hours (Fig. 1A). In addition, caspase-2 processing was not detected in these cells. These observations further confirm that the apoptotic outcome of MC is p53 dependent, and depicts a crucial role for p53 in the regulation of the MC outcome because its deficiency leads to necrosis upon the same treatment (supplementary material Fig. S1B).

To determine the sequence of apoptotic events following MC, siRNA targeting of caspase-2 was performed (Fig. 1C). Similarly to knockdown of p53, cells with reduced caspase-2 levels also underwent MC upon doxorubicin treatment (Fig. 1D). In addition, accumulation of p53 and processing of caspase-8 were still detected in cells lacking caspase-2, indicating that caspase-8 acts upstream of caspase-2 in this experimental system. However, although reduced caspase-2 levels did not change the apoptotic outcome following MC, a delay in this response with respect to caspase-3 processing, as well as the formation of apoptotic bodies, was observed (Fig. 1C,D and supplementary material Fig. S1C,D). This observation is in line with our previous finding in 5-FU-treated wild-type HCT116 cells, in which caspase-2 and caspase-8 were found to operate simultaneously to regulate apoptotic signalling and that knockdown of caspase-2 alone was not sufficient to abolish the apoptotic outcome (Olsson et al., 2009).

Depending on the experimental system used, the involvement of caspases in the development of MC has been variably reported (Castedo et al., 2006; Chan et al., 1999; Nabha et al., 2002; Vakifahmetoglu et al., 2008; Vitale et al., 2005). As for 14-3-3σ-knockout HCT116 cells, caspase-2 has been shown not to be required for cisplatin-induced MC in SKOV-3 cells. However, to rule out any possible involvement of caspases in the development of MC, 14-3-3σ-knockout HCT116 cells were pre-treated with the pan-caspase inhibitor Z-VAD.fmk before doxorubicin exposure. Despite the complete hindrance of caspase-2 and caspase-3 processing and PARP cleavage, indicating an inhibition of caspase activity, multinucleated cells still appeared 16–24 hours following doxorubicin administration (Fig. 1E,F).

Taken together, these results demonstrate that the development of MC occurs independently of the p53 status and any caspase activity. However, the presence of a functional p53 is required for a caspase-mediated apoptotic response following MC.

Cells that undergo MC trigger p53-dependent apoptosis

It is well known that tumour cells differ in their sensitivities to treatment with various chemotherapeutic agents. Upon severe DNA damage, sensitive cells can die by immediate necrosis or apoptosis in the interphase before entering mitosis. Although low doses of such agents are still able to induce an immediate interphase death of some tumour cells, most cells become arrested in the G1–S or G2–M boundaries. Because doxorubicin administration has been reported to induce different modes of cell death dependent on the dosage (Eom et al., 2005; Park et al., 2005; Park et al., 2007), the susceptibility of 14-3-3σ-knockout HCT116 cells to MC upon treatment with low (600 nM) or high (2 μM) doxorubicin doses was investigated. As expected, changes in nuclear morphology and TUNEL-positivity were different and dose-dependent. Cells exposed to high doses showed a time-dependent increase in the number of apoptotic nuclei with condensed chromatin, without any morphological

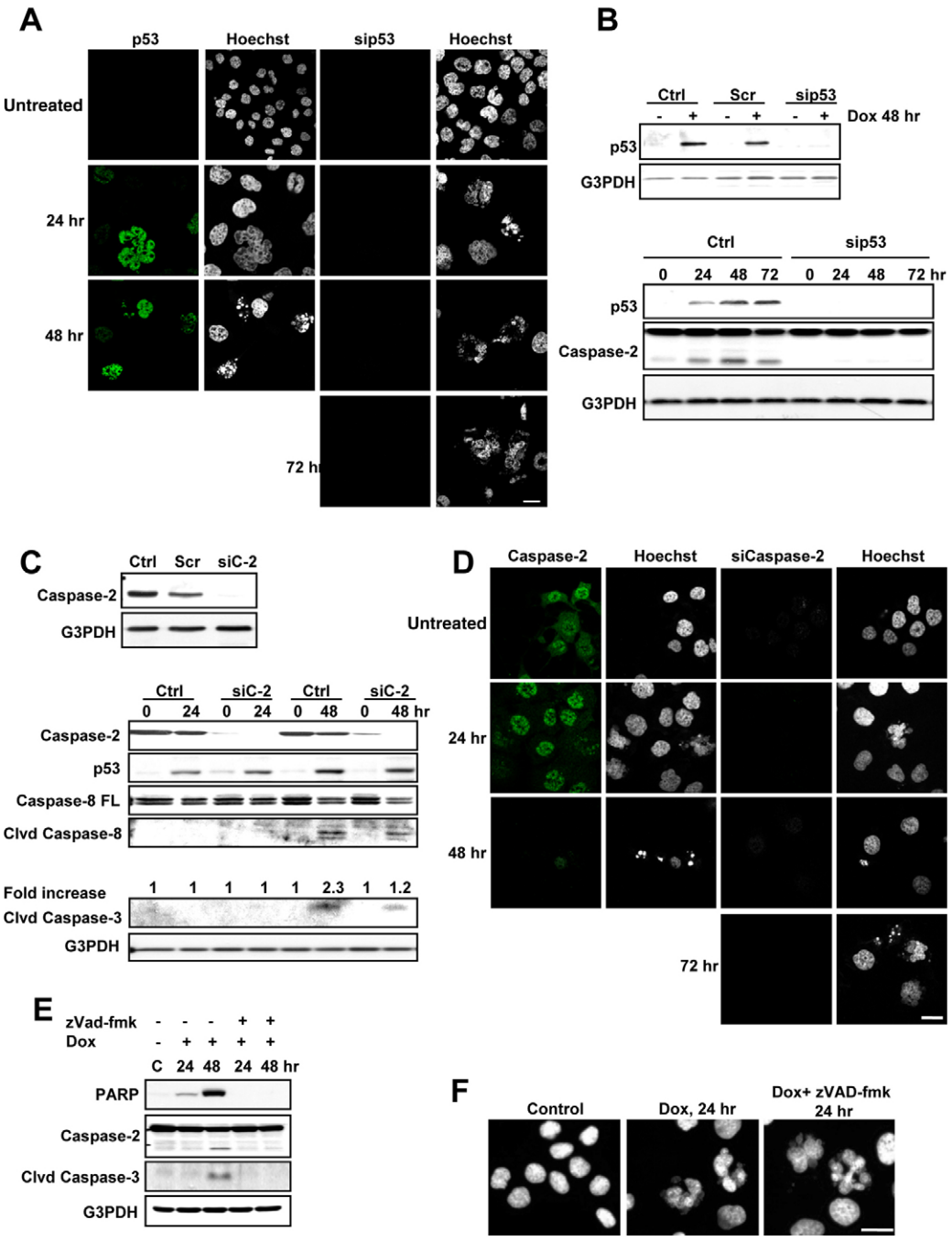

Fig. 1. Regulators of apoptotic outcome following MC. 14-3-3σ-knockout HCT116 cells were cultured and transfected with siRNA to knock down p53 or caspase-2 for 48 hours before doxorubicin (600 nM) treatment. Cell lysates were harvested at indicated time points after treatment and analysed by western blot (50 μg) or immunostaining using antibodies directed against p53 or caspase-2 (green). Scrambled siRNA was used as a control. Blots were reprobed for G3PDH to confirm an equal loading of the samples. Costaining of nuclei was performed using Hoechst 33342 (white). (**A**) Representative confocal images showing the nuclear morphology of untransfected or siRNA-transfected (sip53) cells treated with or without doxorubicin up to 72 hours. (**B**) siRNA silencing of p53 (sip53) at 48 hours after transfection (top). Immunoblots with antibodies against p53 and caspase-2 in control and p53-knockdown cells upon doxorubicin treatment (bottom). (**C**) Immunoblots to detect p53, caspase-2, caspase-3 and caspase-8 in control and caspase-2-knockdown cells 24 and 48 hours after transfection. The cleaved form of caspase-3 was quantified against G3DPH and is presented as fold increase above respective lanes. (**D**) Representative confocal images showing the nuclear morphology of untransfected or caspase-2-knockdown cells treated with or without doxorubicin up to 72 hours. (**E**) Immunoblots of cleaved PARP, caspase-2 and caspase-3 from doxorubicin-treated and z-VAD.fmk-pretreated cells. (**F**) Representative images showing the nuclear morphology of doxorubicin-treated and z-VAD.fmk-pretreated cells visualised using a confocal microscope. Scale bar: 20 μm.

characteristics of MC (Fig. 2A,C). These cells displayed the processing of caspase-2, caspase-3 and caspase-8, as well as PARP cleavage after 16 hours of treatment (Fig. 2B). By contrast, cells treated with low doses of doxorubicin underwent MC before apoptosis (Fig. 2A,C) and displayed a 24 hour delay in apoptotic response compared with cells treated with 2 μM doxorubicin (Fig. 2B,D). Moreover, a pronounced accumulation of p53 was not detected until 24 hours after treatment, during which time, cells had already begun to show MC-associated morphological changes. Notably, only a minor p53 upregulation was detected at high doses of doxorubicin exposure (Fig. 2B). Because no release of lactate dehydrogenase, which is indicative of cell lysis, was detected upon treatment of cells with 2 μM doxorubicin (supplementary material Fig. S2A), a high concentration of doxorubicin seems to induce apoptosis, but not necrosis. Despite the lack of p53 activation, the high-dose doxorubicin-induced apoptotic response involved caspase activation. These results indicate the existence of different mechanisms for initiating an apoptotic response depending on the time of its initiation (before or after MC). Thus, severe DNA damage induced by high doses of doxorubicin activates a p53-independent immediate interphase apoptosis without arresting cells, whereas DNA damage caused by low doses of doxorubicin is not sufficient to kill cells, but rather leads to their arrest at G2. However, the lack of 14-3-3σ impairs the ability to maintain a stable G2 arrest, forcing cells to enter mitosis in the presence of

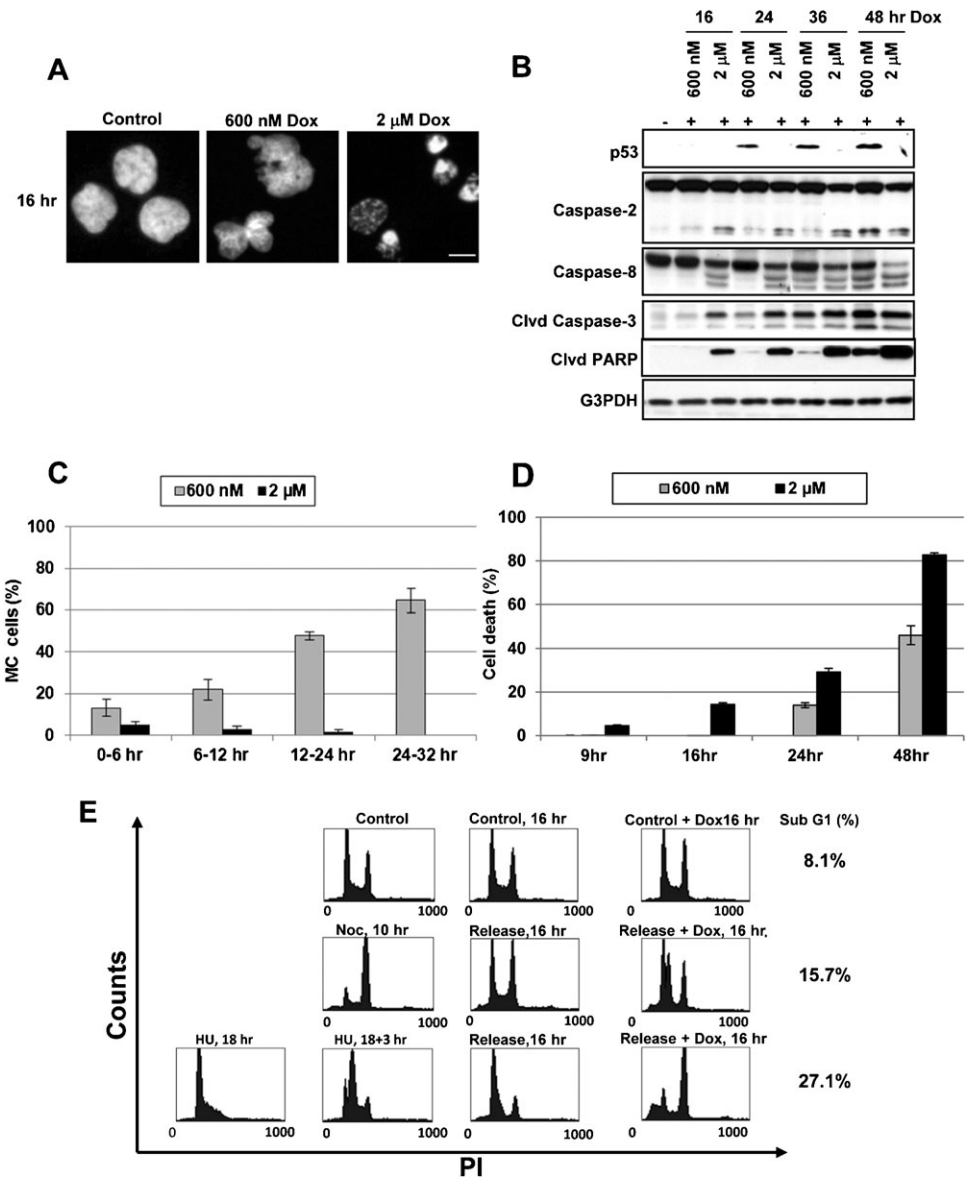

Fig. 2. MC is a prerequisite for triggering p53-dependent apoptosis. Untreated and low-dose (600 nM) or high-dose (2 μM) doxorubicin-treated 14-3-3σ-knockout HCT116 cells were cultured and harvested at indicated time points and analysed by western blot (50 μg), FACScan and nuclei staining. Blots were reprobed for G3PDH to confirm an equal loading of the samples. Nuclei were stained with Hoechst 33342 (white). (**A**) Representative confocal images of nuclear morphology. Condensed nuclei characteristic of apoptosis can be observed only upon treatment with 2 μM doxorubicin. (**B**) Immunoblots to detect p53, caspase-2, caspase-3, caspase-8 and PARP following treatment with low and high doses of doxorubicin. (**C**) Quantification of MC in low- and high-dose doxorubicin-treated 14-3-3σ-knockout HCT116 cells, obtained from live imaging analysis. (**D**) Quantification of cell death using Trypan Blue staining of control and doxorubicin-treated 14-3-3σ-knockout HCT116 cells. Error bars represent the mean of three independent experiments ± s.e.m. (**E**) FACS analysis of the cell cycle distribution after M-phase or G1–S-phase synchronisation and doxorubicin (600 nM) treatment. The sub-G1 population is depicted in the treated samples. Scale bar: 20 μm.

DNA damage and develop MC, after which a p53-dependent apoptosis is initiated. This suggests that the death signal leading to p53 activation is generated during and/or after MC.

To elucidate the possible requirement of an aberrant mitosis to initiate p53-dependent apoptosis, 14-3-3σ-knockout HCT116 cells were synchronised in the M- or S-phases of the cell cycle using nocadazole and hydroxyurea, respectively (Fig. 2E). Cells progressed to MC independently of their cell cycle distribution before doxorubicin treatment (supplementary material Fig. S2B). Notably, those cells synchronised in the S-phase before treatment underwent apoptosis more rapidly than those synchronised in the M-phase, as indicated by the early appearance of the apoptotic bodies and the sub-G1 population observed in flow cytometric analysis (Fig. 2E and supplementary material Fig. S2B). This demonstrates that cells at the S-phase enter premature mitosis and initiate MC, leading to apoptosis faster than cells arrested at the M-phase, which have to progress through a whole cell cycle to enter the next mitosis. This observation further supports our hypothesis that MC is a prerequisite for a p53-dependent apoptotic outcome.

ATM, but not ATR, triggers p53-dependent apoptosis following MC

In addition to its central role in apoptosis induced by DNA damage, our results identify p53 as an important regulator of apoptosis subsequent to MC. Therefore, it was essential to clarify the molecular mechanism underlying p53 activation during this process. ATM–Chk2 and ATR–Chk1 are two of the major DNA-damage-response pathways leading to the activation of p53. Although an ATM–ATR signalling pathway has been implicated in cell death during premature mitosis (Niida et al., 2005), the precise role of these proteins in the process following MC is not described. To determine the possible function of ATM and/or ATR in p53 activation and apoptosis following MC, their expression levels in 14-3-3σ-knockout HCT116 cells were downregulated using siRNA technology. Knockdown of ATM

reduced the level of p53, protected cells against apoptosis and shifted cell death towards necrosis (Fig. 3A,C,E). By contrast, ATR-downregulated cells showed an increased frequency of MC, and underwent apoptosis at earlier time points compared with control cells (Fig. 3D,F).

Once activated, ATM phosphorylates downstream key DNA-damage-response proteins, including Chk2 and H2AX. Mammalian p53 is also a direct target of ATM. γH2AX enables the formation of nuclear foci, sites of DNA damage to which various DNA damage response regulators are recruited. As shown in Fig. 3A, H2AX phosphorylation was increased in a time-dependent manner upon doxorubicin exposure. At 36–48 hours, cells displayed their highest H2AX phosphorylation levels. This increase was delayed in ATM-downregulated cells (Fig. 3A, see quantification), whereas the reduction of ATR seems to lead to a more rapid increase in γH2AX and p53 levels compared with cells treated with doxorubicin alone (Fig. 3B). These results imply a crucial role for ATM in activating p53, but less critical for H2AX phosphorylation, and a requirement for the ATM–p53 pathway of MC to eliminate cells escaping an aberrant mitosis following DNA damage by apoptosis.

Increased H2AX phosphorylation during MC activates the death signal

The phosphorylation of H2AX is one of the major and early responses to DSBs (Fernandez-Capetillo et al., 2003). We

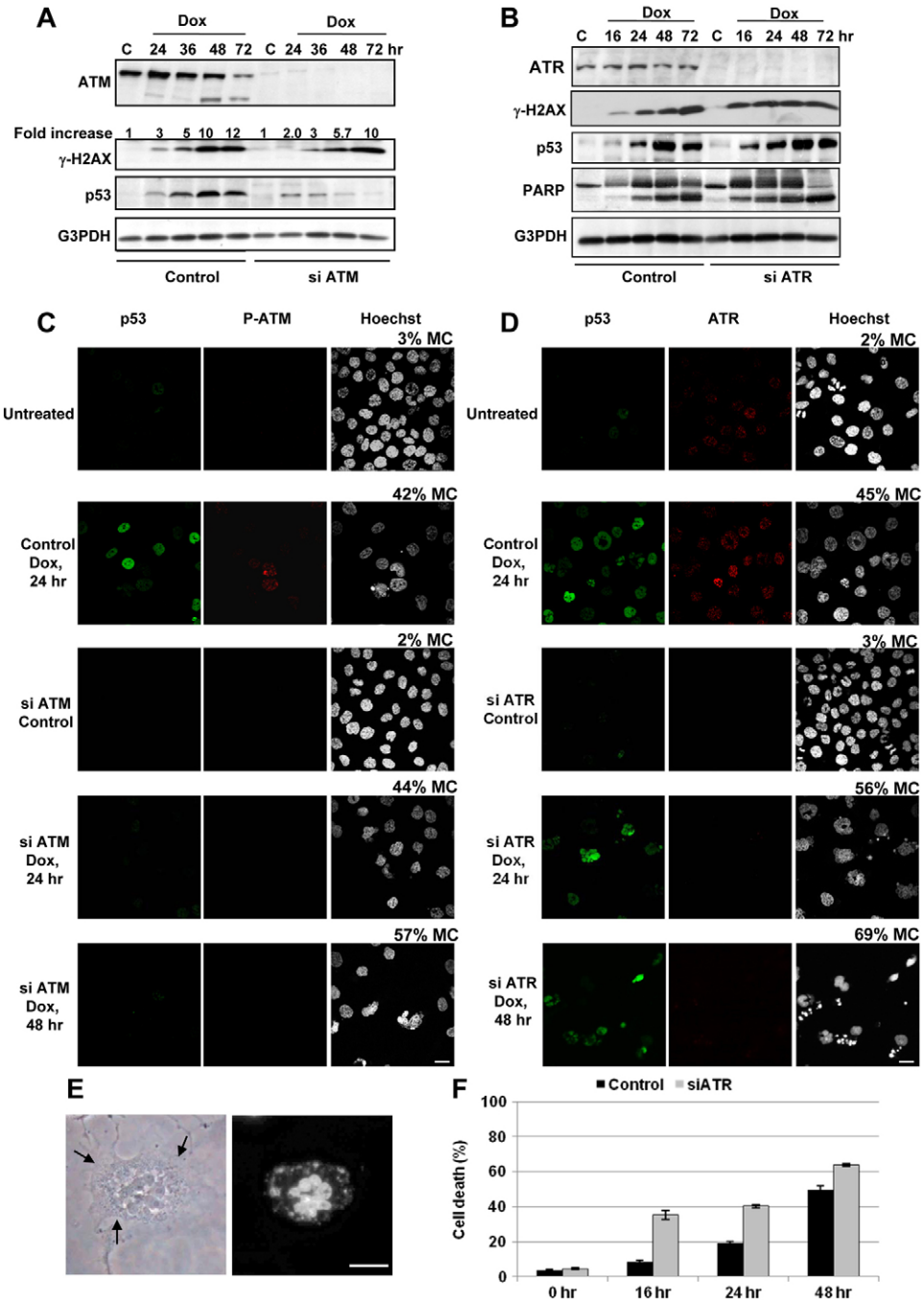

Fig. 3. ATM, but not ATR, is required for the apoptotic outcome following MC. 14-3-3σ-knockout HCT116 cells were cultured and transfected with siRNA to knock down ATM or ATR 48 hours before doxorubicin (600 nM) treatment. Cell lysates were harvested at indicated time points after treatment and analysed by western blot (50 μg) and immunostaining using antibodies directed against p53 (green) or phosphorylated ATM (red) or ATR (red). Scrambled siRNA was used as a control. Blots were reprobed with G3PDH to confirm an equal loading of the samples. The co-staining of nuclei was performed using Hoechst 33342 (white). (**A**) Immunoblots of ATM, γH2AX and p53. (**B**) Immunoblots of ATR, γH2AX, PARP and p53. (**C**,**D**) Representative confocal images showing the nuclear morphology of untransfected cells and cells transfected with siRNA to knock down ATM (C) or ATR (D), with or without doxorubicin treatment. Above each set of images, the percentage of MC cells in one out of three independent experiments is shown. (**E**) Representative image of a cell transfected with siRNA against ATM and treated with doxorubicin for 72 hours, showing a dissolved nucleus and random rupture of the plasma membrane (arrows), typical features of necrotic cells. (**F**) FACS analysis of the cell cycle distribution and quantification of the sub-G1 population in control and in cells transfected with siRNA against ATR after doxorubicin treatment at indicated time points. Error bars represent the mean of three independent experiments ± s.e.m. Scale bar: 20 μm.

observed that in addition to the initial H2AX phosphorylation caused by doxorubicin, an increase in levels of γH2AX started about the same time as MC cells became evident (Fig. 3A,B). Notably, this additional increase occurred concomitantly with the increased level of ATM and p53, but was independent of ATM (Fig. 3A). It is possible that during MC additional DNA strand breaks are generated, which might be the triggering signal for the observed increase in H2AX phosphorylation. To explore this possibility the time dependency of γH2AX following doxorubicin treatment was investigated. The immunostaining of 14-3-3σ-knockout HCT116 cells using an anti-γH2AX antibody revealed a high level of H2AX phosphorylation from 16 hours of exposure onwards compared with the γH2AX level detected at earlier time points (Fig. 4A). Notably, cells undergoing MC displayed a stronger γH2AX signal than cells that are not in MC. Similarly, 5-fluorouracil-treated p53-deficient HCT116 cells also displayed an increase in γH2AX levels as they underwent MC (supplementary material Fig. S3). The increase in γH2AX was not detected in doxorubicin-treated wild-type HCT116 cells (Fig. 4B). Only after 96 hours of continuous doxorubicin exposure could we observe an increase in the phosphorylation of H2AX level in wild-type HCT116 cells. Moreover, we did not detect any rise in γH2AX when the incubation medium was replaced after 9 hours of doxorubicin treatment and cells were allowed to proliferate in normal growth medium (Fig. 4C). Instead, a decrease in H2AX phosphorylation was observed in a time-dependent manner. Although these cells still acquired the initial DNA damage induced by doxorubicin administration, they continued to proliferate and survive. This suggests an important role for the additional γH2AX increase in initiating a death signal.

To investigate whether cells acquired further DSBs during MC, a comet assay was performed to detect the accumulation of DNA damage. The quantitative analysis of the tail moment in the comet assay demonstrated a two-step increase in DNA damage, which flattened after 16 hours of treatment. No further increase in DNA damage was detected at later time points (Fig. 4D). The second increase, observed at and shortly after 16 hours, correlated with enhanced H2AX phosphorylation (Fig. 3A and Fig. 4A,C).

Taken together these observations suggest that the additional increase in γH2AX is generated independently of the direct DNA damage caused by doxorubicin. This additional damage seems to occur during aberrant mitosis and is responsible for triggering an ATM–p53-dependent death signal to eliminate MC cells.

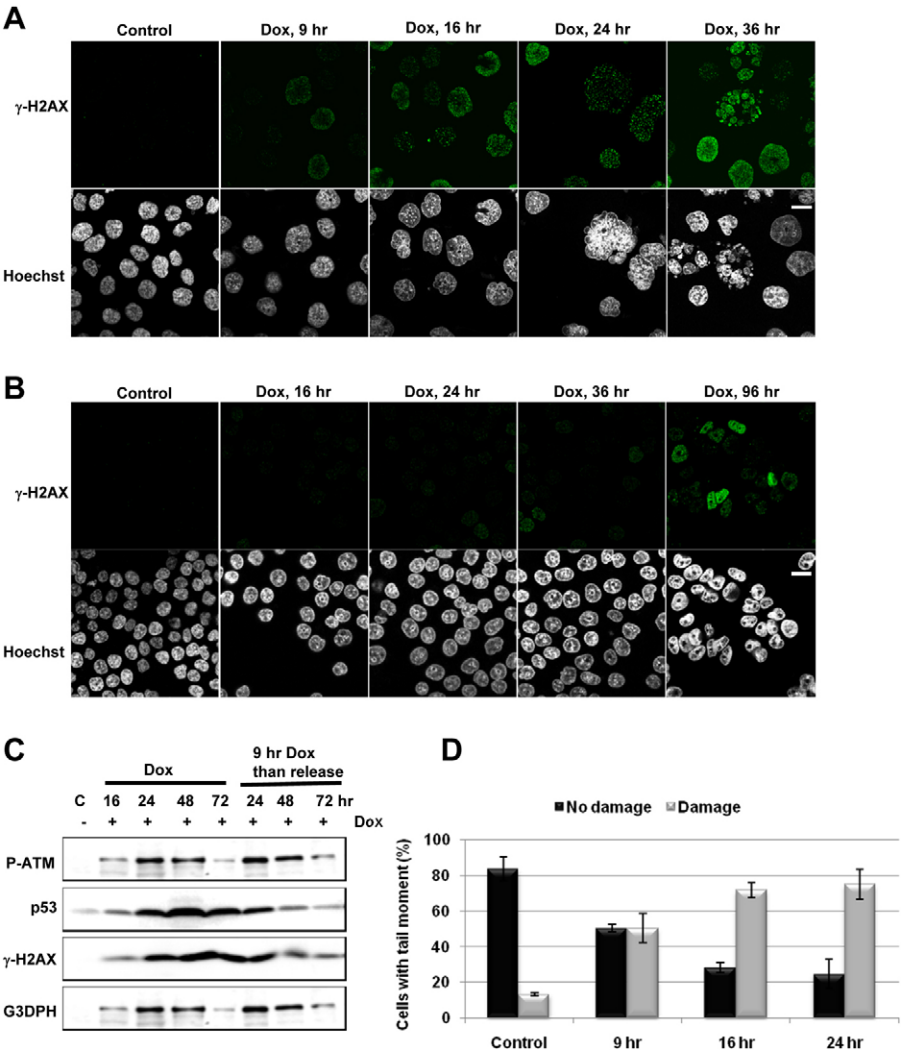

Fig. 4. Increased γH2AX level during MC leads to cell death. Untreated or doxorubicin (600 nM)-treated 14-3-3σ-knockout HCT116 cells were cultured and harvested at indicated time points and analysed by western blot (50 μg), comet assay and immunostaining using antibodies directed against γH2AX (green). Blots were reprobed for G3PDH to confirm an equal loading of the samples. The co-staining of nuclei was performed using Hoechst 33342 (white). (**A**,**B**) Representative confocal images showing nuclear morphology and γH2AX staining in 14-3-3σ-knockout HCT116 (A) or wild-type HCT116 (B) cells after treatment for indicated time. (**C**) 14-3-3σ-knockout HCT116 cells were treated for 9 hours with doxorubicin after which the culture medium was replaced and cells were grown for an additional 24, 48 and 72 hours. Immunoblots of p53, phosphorylated ATM and γH2AX are shown. (**D**) Doxorubicin-induced DNA damage measured by alkaline comet assay. Cells were analysed by fluorescence microscopy and scored according to tail moment. Error bars represent the mean of three independent experiments ± s.e.m. Scale bar: 20 μm.

The apoptotic signal is initiated at the G1–S boundary following mitotic exit

Following a premature mitotic entry, the spindle assembly checkpoint is activated and blocks mitosis progression at the onset of the metaphase–anaphase transition. Although this mitotic arrest is suggested to be associated with apoptosis, our results indicate that MC cells undergo apoptosis following mitotic exit without the completion of cell division (supplementary material Movies 1–3). To find out whether the death signal in 14-3-3σ-knockout HCT116 cells undergoing MC is initiated during mitosis at the stage of mitotic arrest, or after mitotic exit, the status of cyclin B1 as well as of the mitotic checkpoint complex components BubR1, Mad2 and Cdc20 were examined at the time of induction of apoptosis. As shown in Fig. 5A, cells displayed an increase in levels of cyclin B1 16 hours after doxorubicin treatment, about the same time as MC cells started to become evident in the cell population. At later time points, levels of cyclin B1 decreased. Levels of Mad2, BubR1 and Cdc20 protein were also increased 16 hours after doxorubicin administration, but were not sustained at later time points, indicating a transient activation of the spindle checkpoint. Because the degradation of cyclin B1 is regulated by polyubiquitylation in metaphase when the spindle assembly checkpoint is no longer active, our results demonstrate that cells progress through and exit mitosis at the time of the observed decreased level of these proteins. Moreover, because cyclin B1, Cdc20, Mad2 and BubR1 protein levels went down, p53 accumulated and there was a p53-dependent checkpoint response in G1, indicated by an increase in expression of $p21^{CIP1/WAF1}$ after 24 hours (Fig. 5A).

Cells initially arrested at metaphase or anaphase can still complete a catastrophic mitosis and enter G1; however, this occurs without a proper cell division (cytokinesis) and nuclear envelopes form around individual clusters of acentric fragments of lagging or missegregated chromosomes. In this scenario, cells display a multinucleated and/or micronucleated morphology (Erenpreisa et al., 2005). A detailed microscopic investigation of nuclear morphology revealed that doxorubicin-induced MC in 14-3-3σ-knockout HCT116 cells led to an accumulation of cells containing either nuclei united around a single microtubule-organising centre with extensive protrusions or blebs, or several micronuclei, which lacked this connection (Fig. 5B, bottom panel). Although wild-type HCT116 cells are known to arrest at G2–M following DNA damage, a minor fraction of these cells can still enter mitosis in the presence of some chromosomal aberrations before all damage is repaired (probably as a result of insufficient DNA repair) (Fig. 5B, upper panel). Thus, doxorubicin-induced MC in wild-type HCT116 cells leads to the accumulation of cells with different nuclear morphologies than those in doxorubicin-treated 14-3-3σ-knockout HCT116 cells. These cells displayed single nuclei with one or more micronuclei. Chromosomes and chromosome fragments that lag in the interpolar space during anaphase are left outside the daughter nuclei in telophase, which will give rise to a micronucleus distinct from the main nucleus (Fig. 5B, top panel). Moreover, most of these cells survived even several days after treatment, whereas the majority of the multi- and micronucleated cells formed from telophase and cytokinesis failure died by apoptosis following mitotic exit. These morphological differences in MC between wild-type and 14-3-3σ-knockout HCT116 cells might be due to the amount of DNA damage that they repaired before cells entered mitosis. In fact, the cytogenetic analysis of chromosome spread revealed that

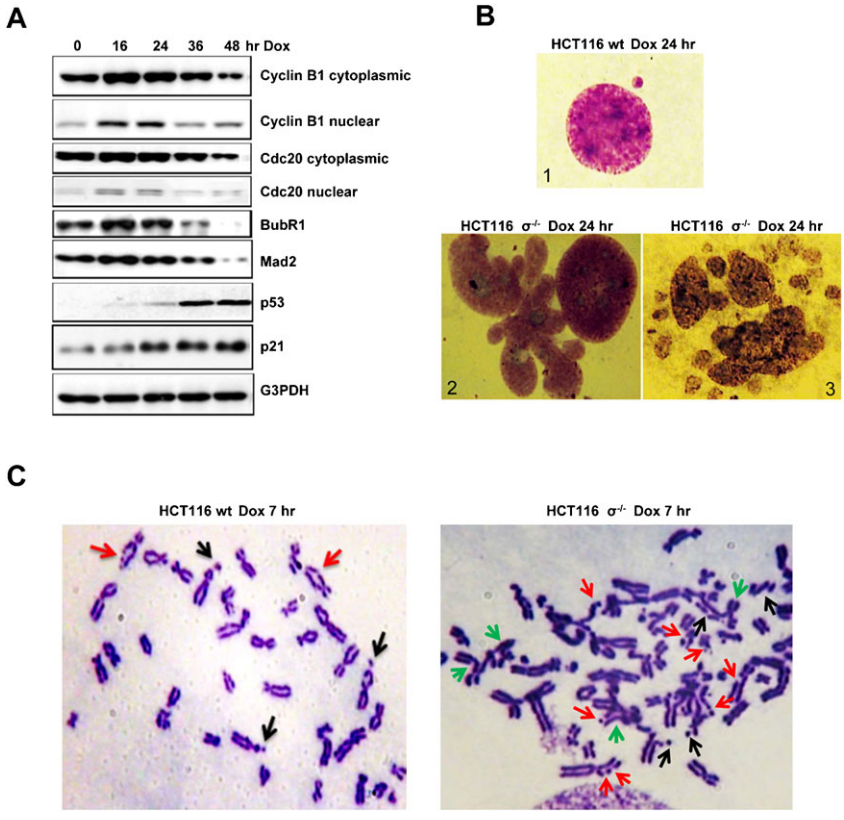

Fig. 5. Doxorubicin treatment of 14-3-3σ-knockout HCT116 cells leads to high-frequency chromatid aberrations and subsequent MC. Untreated or doxorubicin-treated (600 nM) 14-3-3σ-knockout HCT116 cells were cultured and harvested at indicated time points and analysed by western blot (50 μg) and Giemsa staining. (**A**) Immunoblots of cyclin B1, cdc20, Mad2, BubR1, p53 and p21. G3PDH was used as a control for the equal loading of samples. (**B**) Representative Giemsa-stained cytology of MC cells. (1) A solitary micronucleus next to the main nucleus in doxorubicin-treated wild-type HCT116 cells; (2) A multilobular nucleus in treated 14-3-3σ-knockout HCT116 cell undergoing MC (left) compared with a normal nucleus (right); and (3) A 14-3-3σ-knockout HCT116 MC cell displaying lobular nuclear compartments and multiple micronuclei. (**C**) Giemsa staining of chromosome preparations showing chromatid type (G2) aberrations in wild-type HCT116 cells (left) or 14-3-3σ-knockout HCT116 cells (right). Red arrows indicate gaps; black arrows, chromatid fragments; green arrows, exchanges. Right panel shows Giemsa staining of a shattered metaphase in 14-3-3σ-knockout HCT116 cells. Note, the multitude of chromatid gaps breaks and exchanges. Therefore, a successful anaphase is highly unlikely; MC is a predicable outcome of the mitosis. Owing to the abundant number of aberrations, only a few arrows are depicted.

doxorubicin treatment induced chromosomal aberrations (gaps, chromatid and chromosome fragments and chromatid exchanges) in both wild-type and 14-3-3σ-knockout HCT116 cells. However, in wild-type cells, the frequency of chromosome aberrations, although higher than in untreated cells, was relatively low compared with 14-3-3σ-knockout HCT116 cells (Fig. 5C) [wt, 0.27 aberrations per mitosis (n=47); knockout, 7.92 aberrations per mitosis (n=49)]. By contrast, the latter cells displayed a high frequency of chromosome aberrations (almost eight per cell), with double or triple gaps sometimes observed on the same chromatid (Fig. 5C, right panel). Because these cells are not able to arrest in G2–M to repair the damage, they enter mitosis. At the onset of mitosis, a catastrophic division leads to the formation of cells with many distinct micronuclei around a dimorphic nucleus or to a lobular nucleus with protrusions or blebs.

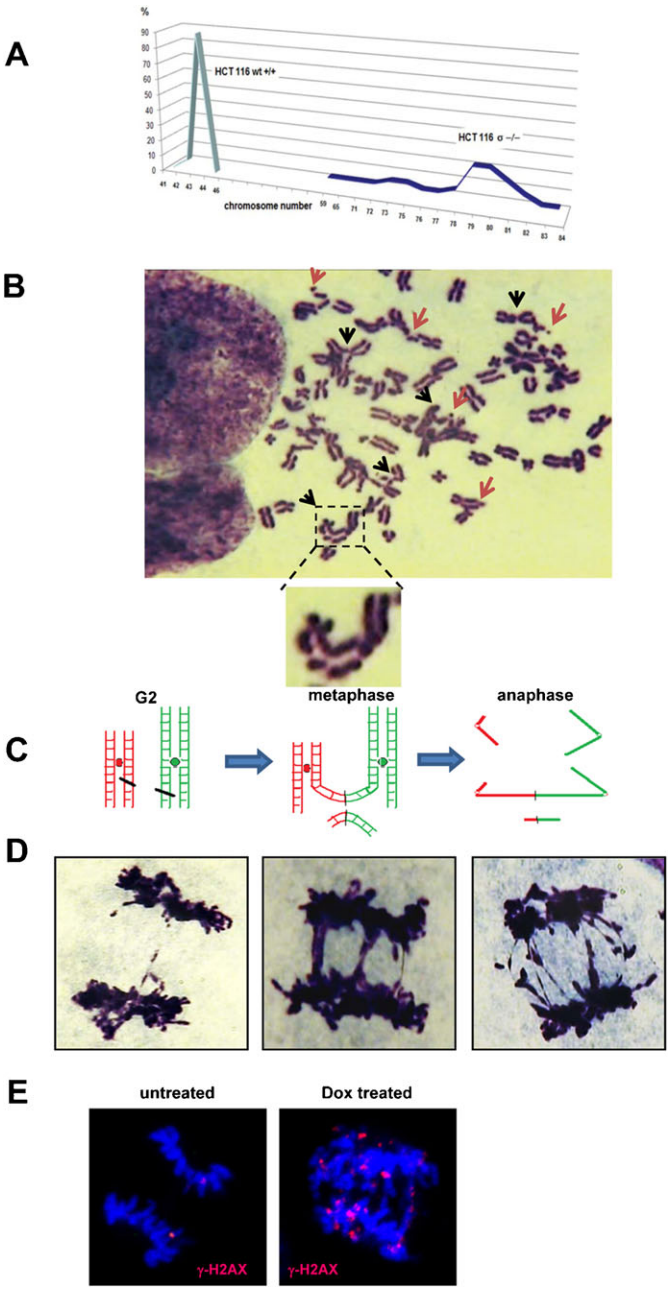

Taken together, these results show that after a transient mitotic arrest doxorubicin-treated 14-3-3σ-knockout HCT116 cells exit mitosis without a proper cell division, displaying a multi- and/or micronucleated morphology because they arrest in G1 by maintaining increased p53 and p21 levels from where they initiate apoptosis.

MC cells acquire additional DNA breaks during anaphase, which are distinct from the initial DSBs caused by doxorubicin

It is known that chromosomal changes or changes in chromatin structure are associated with aberrant mitosis. Therefore, the ploidy status of wild-type and 14-3-3σ-knockout HCT116 cells was analysed by karyotyping. As shown in Fig. 6A, wild-type HCT116 cells represent a clonally selected hypodiploid cell line with a karyotype composed of several rearranged marker chromosomes, as described previously (Roschke et al., 2002). It is a chromosomally stable cell line with a modal number of 44 chromosomes in 85% of mitoses scored. By contrast, 14-3-3σ-knockout HCT116 cells are hypotetraploid cells, with a mean chromosome number of 79–80. The flattened chromosome number frequency curve of these cells with the lack of a dominant subpopulation represents extensive chromosomal instability (Fig. 6A). It seems that the loss of 14-3-3σ influences the type and frequency of chromosomal aberration. Moreover, 14-3-3σ-knockout cells appear to be more susceptible to acquiring DSBs when treated with doxorubicin compared with wild-type cells (Fig. 5C). However, although these cells display a high frequency of chromatin aberrations, the cytogenetic analysis of mitotic chromosomes demonstrates that even in the absence of a proper G2 checkpoint (a period that is essential for successful DNA repair), a large number of cells still attempt to repair these chromosomal aberrations or rejoin chromosome fragments before proceeding into mitosis. Several end-to-end chromosome fusions, many of them of the interchromosomal exchange type that connect two or more chromosomes, as shown by the large frequency of tri- and/or tetraradials, have occurred, most likely during the late-G2 phase (Fig. 6B). These chromosomes usually display two or more centromeres. The different sizes of multicentric chromosomes might have been generated from fusion between a broken end of one chromosome and de novo

Fig. 6. Secondary DNA damage, including broken anaphase bridges, can occur during stressful mitosis. (**A**) Chromosome numbers (% of metaphases counted) in wild-type and 14-3-3σ-knockout HCT116 cell lines. (**B**) Giemsa staining of 14-3-3σ-knockout HCT116 cells showing multiple chromosome aberrations induced by doxorubicin. Multiple gaps, chromatid fragments (red arrows) as well as interchromosomal exchange type aberrations (chromatid translocations) and chromosomes with two or more centromers (black arrows) are observed. (**C**) Schematic representation of a typical break–fusion–bridge (BFB) cycle, which in this particular case starts with a chromatid interchange that leads to an anaphase bridge. (**D**) Giemsa staining of 14-3-3σ-knockout HCT116 cells showing multiple G2 aberrations generating single or multiple anaphase bridges. Left, anaphase bridge broken twice and a second bridge that broke earlier. Middle, a sheaf containing at least three bridges (two are about to break) and a second double bridge (one broken already). A fourth single bridge is on the verge of breaking. Right, multiple broken anaphase bridges and several lagging fragments in an anaphase that will lead to one or two nuclei with a typical lobular MC nuclear morphology flanked by micronuclei. (**E**) Representative confocal images of control or doxorubicin-treated anaphase cells stained for γH2AX (pink) and DNA (blue), suggesting intramitotic (anaphase) signalling.

DSBs on other chromosomes, leaving the remaining parts as new separated fragments that could be potential candidates for additional rearrangements.

Many of the multicentric chromosomes resulted in the formation of anaphase bridges during mitosis (Fig. 6C). These bridges are formed when polycentric chromosomes are stretched between the spindle poles during anaphase. When pulled in opposite directions by the spindle apparatus, the asymmetrical breakage of anaphase bridge chromosomes generates numerous DSBs (Fig. 6D). Doxorubicin-treated 14-3-3σ-knockout HCT116 cells displayed multiple broken bridges almost in all anaphase–telophases scored (anaphases with bridges, 96%; anaphases with broken bridges, 75%; number of bridges per anaphase, 3.1; number of broken bridges per anaphase, 1.9), suggesting an increased amount of DSBs and a generation of the additional DNA-damage signal essential for the initiation of apoptosis. To find out whether enduring DSBs generated during asymmetrical breaks or if anaphase bridges were the cause for the increased level of γH2AX during mitosis, untreated and doxorubicin-treated 14-3-3σ-knockout HCT116 cells were immunostained for γH2AX, and cells in anaphase were examined. In treated cells, which displayed many anaphase bridges, intense γH2AX foci were detected (Fig. 6E). These anaphase bridges do in fact increase the amount of DNA damage by introducing an unexpected source of DNA breaks in a phase of cell cycle when otherwise the tightly condensed chromatin is not open to any external harm. Thus, these bridge breaks are not caused by doxorubicin treatment itself, but are rather additional damage caused by the mechanical force created during the anaphase–telophase migration.

Overall, these observations indicate that break–fusion–bridge chromosome cycles during MC might be the main cause for the increased H2AX phosphorylation that is distinct from those generated from doxorubicin treatment alone. This secondary DNA or chromatin damage generates the transduction of a death signal, whereby many of the initial DNA aberrations end up in anaphase bridges that are continuously breaking. However, we cannot completely exclude the possibility that the initiation of H2AX phosphorylation signalling might start to occur at earlier stages during MC.

Discussion

In this study, we investigated the mitotic events during MC leading to p53-dependent apoptosis. It should be noted that although 14-3-3σ-knockout HCT116 cells contain functional p53, they do not activate it until cells progress through mitosis (see MC development followed by apoptosis in supplementary material Movies 1–3). Hence, doxorubicin-induced DNA damage per se does not trigger a death signal. Exposure to only high doses of doxorubicin generates a sufficient amount of damage to cause immediate interphase cell death. However, at such doses, MC was never observed, and apoptosis progressed independently of p53 activation.

Doxorubicin is a commonly used chemotherapeutic agent in cancer therapy with a complex mechanism of action that is not fully understood. It is known to inhibit DNA biosynthesis, intercalate with DNA and lead to the inhibition of topoisomerase II, which unwinds DNA for transcription. This leads to the prevention of DNA strand separation and causes replication stall forks, generating single-strand breaks and DSBs during late S phase and/or at G2 phases of the cell cycle (Momparler et al., 1976). Mitochondria have been suggested as the primary target of high-dose and/or long-term doxorubicin treatment, with the consequences of generation of reactive oxygen species (ROS), oxidative stress and mitochondrial dysfunction (Green and Leeuwenburgh, 2002). Similarly to our observations (data not shown), in doxorubicin-treated cardiac cells, generation of mitochondrial ROS precedes Bax activation, the loss of mitochondrial membrane potential, release of cytochrome c and subsequent caspase activation (Spallarossa et al., 2004; Tsang et al., 2003; Wang et al., 2001). These data support the notion of an acute cellular response to high doses of doxorubicin that involves mitochondria to induce cell death and accounts for the p53-independent apoptosis observed in 14-3-3σ-knockout HCT116 cells.

Several studies have demonstrated that apoptosis is not the primary response of low-dose doxorubicin treatment. It has been shown that doxorubicin induces two modes of cell death depending on cell type and concentration used (Eom et al., 2005). The inability of 14-3-3σ-knockout HCT116 cells to sequester cyclin B and Cdc2 in the cytoplasm following low-dose doxorubicin-induced DNA damage was used as a convenient MC model (Chan et al., 1999). Cells with impaired or lost checkpoint functions, such as 14-3-3σ-knockout HCT116 cells, are unable to maintain a G2–M arrest and enter mitosis in the presence of unrepaired DNA (Bunz et al., 1998; Kil et al., 2008; Kodym et al., 2008; Radford and Murphy, 1994). The consequence of this mitosis depends on several parameters. Thus, wild-type HCT116 cells survive an aberrant mitosis and die only after several mitotic cycles. Depending on the severity of DNA damage, premature mitosis leads to MC followed by cell death, which occurs either during or after the exit from mitosis at a second arrest at G1. Owing to the lack of a 14-3-3σ protein, MC results from a combination of a deficient G2–M checkpoint and doxorubicin-induced DNA damage. The failure of cell cycle arrest before mitosis triggers an aberrant chromosome segregation, which culminates in the activation of an apoptotic default pathway after mitotic exit. Thus, 14-3-3σ-deficient cells survive through an abnormal mitosis even in the presence of DNA damage, demonstrating that doxorubicin per se does not cause the triggering of an apoptotic signal. Instead, only cells that progress through a catastrophic mitosis undergo apoptosis, emphasising MC as a prerequisite for a p53-dependent apoptotic outcome.

The fact that cells initiated a p53 signal following MC prompted us to investigate at which step during a catastrophic mitosis the death signal is triggered and what the mechanism of this process is. An apoptotic signal can be initiated from mitotic arrest during the metaphase–anaphase transition. However, instead of p53, p73 has been proposed to induce mitotic-linked cell death (Niikura et al., 2007; Toh et al., 2010). Moreover, during mitotic arrest, the activation of p53 occurs in an ATM–ATR-independent fashion. We observed that the doxorubicin-induced DNA damage acquired in interphase was expanded in mitosis, leading to the activation of the mitotic checkpoints. After a transient mitotic arrest, doxorubicin-treated cells exit mitosis without a proper cell division, displaying a multi- and/or micronucleated morphology, and halted in G1. The immediate induction of p21 after mitotic exit is an indicator of a p53-dependent checkpoint response in G1. This acts as a second ‘fail-system’ after an aberrant mitosis (Fig. 7). Notably, the transient activation of spindle checkpoint components Mad2 and BubR1

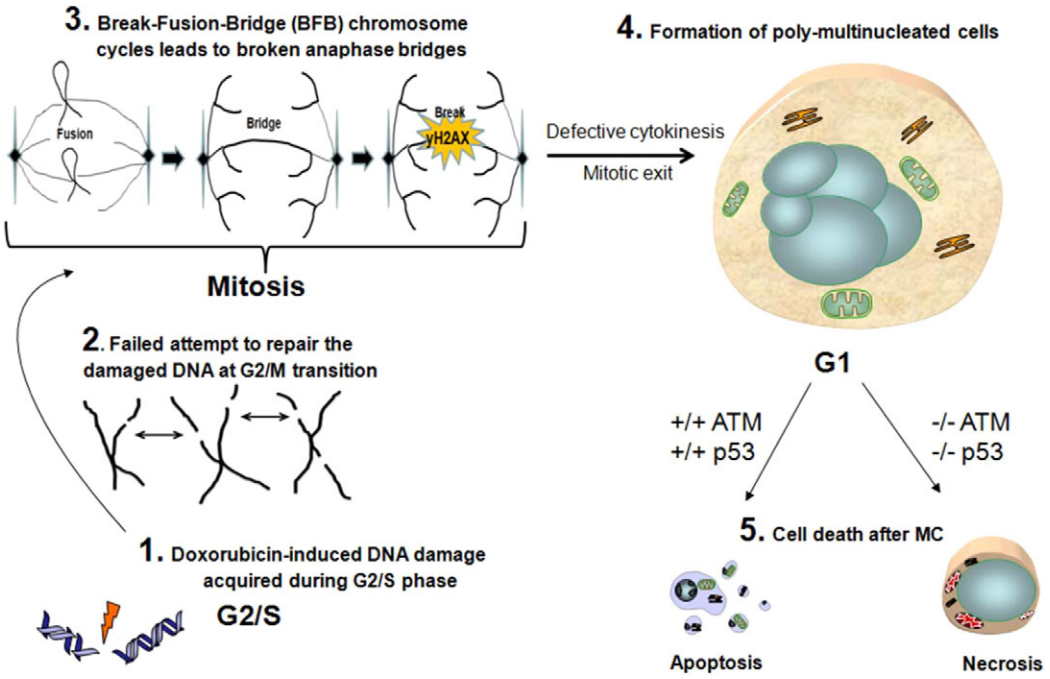

Fig. 7. Schematic representation of the chain of events starting from doxorubicin-mediated DNA damage leading to various modes of cell death after mitotic catastrophe. For details, see Discussion.

revealed that MC progressed independently of mitotic checkpoint function.

During MC, an aberrant mitosis might result in the failure of proper chromatin compaction, as well as errors in chromosome alignment or segregation. These defects can be sensed as a DNA-damage signal and might activate ATM. Moreover, the uncoupling of the onset of mitosis from the completion of DNA replication might also trigger a damage signal that activates ATR. The depletion of ATM and ATR has been suggested to inhibit cell death resulting from a premature mitosis (Niida et al., 2005). In our experimental system, downregulation of only ATM, not ATR, protected against apoptosis. However, it did not protect MC cells from undergoing cell death, but rather switched the cell death to necrosis. Precisely how the activation of ATM is regulated and what signals are involved remains to be investigated.

Although ATM and ATR might share many of the same substrates, drastically different phenotypes have been observed when either of these kinases are knocked down (Brown and Baltimore, 2000; de Klein et al., 2000; Kastan and Lim, 2000). The inability of cells to respond efficiently to DNA strand breaks is associated with the absence of ATM. By contrast, the disruption of ATR leads to early embryonic death, which is associated with extensive chromosomal fragmentation, similarly to that observed when somatic cells undergo premature mitosis (Waldman et al., 1996). The primary role of ATR is to respond to the DNA damage encountered during the S-phase that culminates in replication fork stalling. The immunodepletion of ATR from *Xenopus* extracts was found to cause premature entry into mitosis, even when DNA replication was undisturbed (Hekmat-Nejad et al., 2000). Doxorubicin-treated 14-3-3σ-knockout HCT116 cells with downregulated ATR underwent early MC and apoptosis, compared with control or ATM-downregulated cells. The fact that doxorubicin induces replication damage that would primarily require an ATR-dependent cell cycle arrest via Chk1 supports the assumption that in the experimental system described here, ATR is a direct regulator of mitotic entry. Moreover, because cells with depleted Chk1 were shown to fail to activate the spindle checkpoint, progression through mitosis and exit would occur more rapidly to initiate apoptosis. Hence, the elimination of ATR results in enhanced MC and the loss of mitotic checkpoint control, leading to activation of p53. This might lead to a novel concept, i.e. that replication checkpoint signalling is constitutive rather than induced. This means that the signals recognised by ATR are always present when cells are undergoing DNA replication and that the presence of ATR is required to prevent MC.

MC appeared to be coupled to H2AX phosphorylation and foci formation independently of doxorubicin-induced DNA damage. γH2AX is required for proper mitotic chromatin condensation (Fernandez-Capetillo et al., 2003; Ichijima et al., 2005). Recently, it was shown that MC induced by depletion of histone acetyltransferase was followed by H2AX phosphorylation and foci formation independently of DNA damage (Ha et al., 2009). We have observed that additional DNA damage occurred subsequent to mitotic entry, which is distinct from that initially produced by doxorubicin. Although incapable of maintaining a G2–M arrest, a large amount of 14-3-3σ-knockout HCT116 cells still attempt to repair DNA damage by the rejoining and/or end-to-end joining of chromosomes or fragments before proceeding into mitosis. In MC, as in mitotic cells, chromosomes are tightly packed, which can affect the accessibility of DNA repair factors to damage sites. Hence, homologue recombination or even DNA end joining cannot occur efficiently. These unsuccessful attempts to repair result in breakage–fusion–bridge (BFB) chromosome cycles, giving rise to additional DNA damage. These data verify

a novel mechanism for the generation of DNA damage during MC. Furthermore, the level of γH2AX increased and persisted regardless of the initial damaging stimuli, indicating the inability to repair and switch off the repair signal for the death signal. Thus, we propose that an increased level of γH2AX is a sign of the second, indirect chromosomal damage acquired during MC (Fig. 7). This increase triggers a DNA-damage response by an ATM–p53-dependent apoptotic signalling pathway, leading to the elimination of MC cells and acting as a second 'fail-system' after an aberrant mitosis. Thus, in cells that contain defective G2–M checkpoints, MC seems to represent an additional mechanism to prevent genomic instability.

Even in the absence of DNA damage, the phosphorylation of H2AX in normal cell cycle progression might contribute to the maintenance of genomic integrity. In unstressed conditions, the downregulation of Chk1 in osteosarcoma results in premature mitotic entry and increased γH2AX levels, leading to apoptosis at later time points (Carrassa et al., 2009). Interestingly, the γH2AX level changed throughout cell cycle progression in proliferating cells, and was maximal in the M phase. Furthermore, the phosphorylation of H2AX during mitosis was shown to be dependent on ATM but not on DNA-dependent protein kinase (DNA-PK) (Giunta et al., 2010). However, we found that the rise in γH2AX levels was delayed in ATM-downregulated cells. By contrast, in ATR-downregulated cells, γH2AX levels increased at earlier time points upon doxorubicin treatment. The possibility that DNA-PK is responsible for the DNA repair attempts through non-homologous end joining (NHEJ) and for the increased γH2AX level in 14-3-3σ-knockout HCT116 cells exists. Although the molecular mechanism regulating H2AX phosphorylation during MC requires further clarification, our data support the idea of a crucial role for increased H2AX phosphorylation in determining elimination of cells with MC.

It has become clear that following treatment with chemotherapeutic drugs, tumour cells can be eliminated by MC, and the failure to undergo MC has been suggested to contribute to tumorigenesis. As an alternative, we propose that, in response to chemotherapeutic drugs, cells undergo MC and then either survive and develop cancer, or die by apoptosis or necrosis. Accumulating evidence has suggested that H2AX phosphorylation is the determining factor between initiation of cell death and survival. It is widely accepted that unrepaired or misrepaired DNA DSBs lead to the formation of chromosomal aberrations. Consequently, when cells undergo improper mitosis, multiple bridges and multiple lagging fragments are formed. Accumulation of γH2AX during MC might represent a possible anticancer mechanism to prevent the survival of chromosomally unstable cells. Accordingly, a novel concept of cancer treatment targeting MC is emerging.

Materials and Methods

Cell culture

The 14-3-3σ-knockout HCT116 cells (gift from Bet Vogelstein, Johns Hopkins Kimmel Cancer Center, Baltimore, MD) were cultured in McCoy's medium supplemented with 10% (w/v) heat-inactivated foetal calf serum and geneticin 400 μg/ml. Wild-type HCT116 cells were cultured in DMEM medium supplemented with 10% (w/v) heat-inactivated foetal calf serum, 100 U/ml penicillin and 100 μg/ml streptomycin. Cells were grown in a humidified 5% CO_2 atmosphere at 37℃ and maintained in a logarithmic growth phase for all experiments. Throughout the experiments (if not stipulated otherwise) cells were treated with 600 nM doxorubicin (Teva, Sweden) for the indicated time periods. In selected samples, the caspase inhibitor z-VAD-fmk (10 μM) or z-VDVAD-fmk (10 μM) (Enzyme Systems Products, Livermore, CA) was added 30 minutes before treatment with the chemotherapeutic drug. For synchronisation in the G2–M phase, cells were treated for 10 hours with nocodazole (40 ng/ml). The G2–M cells were then collected, washed three times with PBS, replated and treated with doxorubicin for the indicated time periods. For S-phase synchronisation, cells were treated with hydroxyurea (2 mM) for 12 hours, washed three times with PBS and released for an additional 3 hours before the addition of doxorubicin for the indicated time periods. For FACS analysis, cells were harvested at the indicated time points, fixed in 70% ethanol overnight and stained with propidium iodide (PI) solution [50 mg PI/ml, 0.1% (w/w) Triton X-100 and 0.1% (w/w) Na-citrate in PBS] in the presence of RNase A (0.5 mg/ml at 37℃ for 30 minutes). Flow cytometric analysis was carried out using a FACScan flow cytometer equipped with CellQuest software (Becton Dickinson, San Jose, CA).

Cytogenetic analysis

Cytogenetic analysis was performed on wild-type and 14-3-3σ-knockout HCT116 cells 7 hours after doxorubicin treatment. At the end of this period, a 1.5 hour colcemid treatment (0.1 μg/ml; KaryoMax Colcemid, GIBCO) allowed chromosome spreading. Chromosome preparations were made according to a standard air-drying procedure including treatment for 20 minutes with 0.075 M KCl hypotonic and glacial acetic acid: methanol 1:3 fixation. The slides were stained with Giemsa and analysed at 1000× magnification.

Hoechst staining and immunofluorescence

Cells seeded overnight on coverslips were fixed for 20 minutes in 4% paraformaldehyde on ice. The permeabilisation and blocking of nonspecific binding of antibodies were performed by the incubation of cells in PBS buffer containing 10 mM HEPES, 3% BSA and 0.3% Triton X-100 at room temperature for 60 minutes. Incubations with primary and secondary antibodies diluted in 1% BSA (PBS buffer) were performed at 4℃ overnight or at room temperature for 60 minutes, respectively. The counterstaining of nuclei was carried out by incubation for 10 minutes with Hoechst 33342 (1 μg/ml in PBS solution) at room temperature. Between all steps, cells were washed three times for 5 minutes with PBS. Stained sections were mounted using Vectashield H-1000 (Vector Laboratories) and examined either under an LSM 510 META confocal laser scanner microscope (Zeiss, Göttingen, Germany) or fluorescence microscope (Nikon ECLIPSE TE2000-S, Nikon, Kanagawa, Japan). Fluorescent secondary antibodies directed to mouse (Alexa Fluor 488) and rabbit (Alexa Fluor 594) IgG were purchased from Molecular Probes (Leiden, The Netherlands).

Live-cell imaging

Cells were grown on 12-well cell culture plates at 37℃ in a 5% CO_2 incubation chamber. McCoy's cell medium (supplemented as mentioned above) was used during image acquisition, with a layer of mineral oil on top of the medium to prevent evaporation. All images were collected with a Nikon TE2000E Automated Inverted Microscope equipped with 40× Plan Apo, NA 1.2 objective lens and the Perfect Focus System for continuous maintenance of focus. Images were acquired with a Hamamatsu ORCA ER cooled CCD camera controlled with MetaMorph 7 software and collected every 20 minutes. Gamma, brightness and contrast were adjusted on displayed images using MetaMorph 7 software.

Gel electrophoresis and immunoblotting

Cell were harvested, washed in PBS and lysed for 10 minutes at room temperature in lysis buffer supplemented with complete protease inhibitors (Roche Diagnostics). Cell extracts were centrifuged at 13,000 rpm for 10 minutes at 4℃ to separate the insoluble material, followed by a determination of protein concentration using the BSA assay (Pierce). Equal amounts of protein from each sample were mixed with Laemmli loading buffer, boiled for 5 minutes and subjected to SDS-PAGE. Membranes were blocked for 1 hour with 5% non-fat milk in PBS at room temperature and subsequently probed with the primary antibody of interest. Blots were revealed by ECL™ (Amersham Biosciences, Uppsala, Sweden).

Antibodies

Primary antibodies used in western blotting and immunostaining were as follows: anti-p53 mAb, (BD Biosciences); anti-p53 mAb (Santa Cruz); anti-phosphorylated p53 (Ser15) (Cell Signalling) anti-cleaved caspase-3 clone Asp175 (Cell Signaling); polyclonal anti-caspase-8 (BD Biosciences); anti-caspase-2 (BD Biosciences); polyclonal anti-GAPDH (Nordic Biosite, Täby, Sweden); polyclonal anti-phosphorylated H2AX (Cell Signaling), anti-PARP (BD Biosciences); anti-cleaved PARP mAb (Cell Signaling), anti-BubR1 and anti-Mad2 (Santa Cruz), anti-Cyclin B1 and anti-Lamin B1 (Santa Cruz) and anti-ATM and anti-ATR mAbs (Cell Signaling). Horseradish peroxidase-conjugated secondary antibodies were purchased from Pierce.

siRNA methodology

Silencing of mRNA encoding caspase-2, p53, ATM and ATR was achieved by the transfection of 21 nt RNA duplexes using Interferin (Polyplus Transfection) reagent according to the manufacturer's instructions and using 10 nM of

double-stranded siRNA (caspase-2 and p53) (Qiagen) and 50 nM (ATM, ATR) (Dharmacon). The level of expression of caspase-2, p53, ATM and ATR in targeted cells was monitored by SDS-PAGE and immunohistochemistry.

Comet assay

The comet assay was performed using the method described earlier with some modifications (Sasaki et al., 1997). Briefly, cells were exposed to 600 nM doxorubicin for 9, 16 and 24 hours. At the end of the incubation, cells were removed from the plates with trypsin, washed and diluted in 70 µl low-melting-point agarose (0.75% w/v in PBS). The resulting suspensions were embedded in previously prepared normal-melting-point agarose (1% w/v in PBS) on frosted slides. The slides were then immersed in lysis buffer (2.5 M NaCl, 100 mM sodium-EDTA, 10 mM Tri-HCl, pH 10) for 1 hour at 4℃ in the dark. After lysis, slides were placed in alkaline electrophoresis buffer (0.3 M NaOH, 1 mM sodium-EDTA) for 20 minutes at 4℃ to denature DNA and express alkali-labile sites. Electrophoresis was carried out at 4℃ for 10 minutes at 1.6 V/minute. The slides were then washed twice in neutralising buffer (0.4 M Tris-HCl, pH 7.4) for 5 minutes. DNA was stained with ethidium bromide (20 µg/ml) per slide. More than 100 nuclei on each slide were examined for the presence of comet tails at 200× magnification. Comet images were analysed using CometScore software (TriTek Corporation), and the tail moment was used as the primary measurement for the quantification of DNA damage.

We thank Bert Vogelstein for wild-type and 14-3-3$\sigma^{-/-}$ HCT116 cells, Alena Vaculova for technical support. This work was supported by grants from the Swedish Research Council, the Swedish and the Stockholm Cancer Societies, the Swedish Childhood Cancer Foundation, Swedish Society for Medical Research, the EC FP-6 (Chemores) as well as the FP7 (APO-SYS) programs.

Supplementary material available online at
http://jcs.biologists.org/lookup/suppl/doi:10.1242/jcs.081612/-/DC1

References

Brown, E. J. and Baltimore, D. (2000). ATR disruption leads to chromosomal fragmentation and early embryonic lethality. *Genes Dev.* **14**, 397-402.

Bunz, F., Dutriaux, A., Lengauer, C., Waldman, T., Zhou, S., Brown, J. P., Sedivy, J. M., Kinzler, K. W. and Vogelstein, B. (1998). Requirement for p53 and p21 to sustain G2 arrest after DNA damage. *Science* **282**, 1497-1501.

Carrassa, L., Sanchez, Y., Erba, E. and Damia, G. (2009). U2OS cells lacking Chk1 undergo aberrant mitosis and fail to activate the spindle checkpoint. *J. Cell. Mol. Med.* **13**, 1565-1576.

Castedo, M., Coquelle, A., Vivet, S., Vitale, I., Kauffmann, A., Dessen, P., Pequignot, M. O., Casares, N., Valent, A., Mouhamad, S., Schmitt, E., Modjtahedi, N., Vainchenker, W., Zitvogel, L., Lazar, V., Garrido, C. and Kroemer, G. (2006). Apoptosis regulation in tetraploid cancer cells. *EMBO J.* **25**, 2584-2595.

Castedo, M., Perfettini, J. L., Roumier, T., Valent, A., Raslova, H., Yakushijin, K., Horne, D., Feunteun, J., Lenoir, G., Medema, R. et al. (2004a). Mitotic catastrophe constitutes a special case of apoptosis whose suppression entails aneuploidy. *Oncogene* **23**, 4362-4370.

Castedo, M., Perfettini, J. L., Roumier, T., Yakushijin, K., Horne, D., Medema, R. and Kroemer, G. (2004b). The cell cycle checkpoint kinase Chk2 is a negative regulator of mitotic catastrophe. *Oncogene* **23**, 4353-4361.

Chan, T. A., Hermeking, H., Lengauer, C., Kinzler, K. W. and Vogelstein, B. (1999). 14-3-3Sigma is required to prevent mitotic catastrophe after DNA damage. *Nature* **401**, 616-620.

de Klein, A., Muijtjens, M., van Os, R., Verhoeven, Y., Smit, B., Carr, A. M., Lehmann, A. R. and Hoeijmakers, J. H. (2000). Targeted disruption of the cell-cycle checkpoint gene ATR leads to early embryonic lethality in mice. *Curr. Biol.* **10**, 479-482.

Eom, Y. W., Kim, M. A., Park, S. S., Goo, M. J., Kwon, H. J., Sohn, S., Kim, W. H., Yoon, G. and Choi, K. S. (2005). Two distinct modes of cell death induced by doxorubicin: apoptosis and cell death through mitotic catastrophe accompanied by senescence-like phenotype. *Oncogene* **24**, 4765-4777.

Erenpreisa, J., Kalejs, M. and Cragg, M. S. (2005). Mitotic catastrophe and endomitosis in tumour cells: an evolutionary key to a molecular solution. *Cell Biol. Int.* **29**, 1012-1018.

Fernandez-Capetillo, O., Mahadevaiah, S. K., Celeste, A., Romanienko, P. J., Camerini-Otero, R. D., Bonner, W. M., Manova, K., Burgoyne, P. and **Nussenzweig, A**. (2003). H2AX is required for chromatin remodeling and inactivation of sex chromosomes in male mouse meiosis. *Dev. Cell* **4**, 497-508.

Gewirtz, D. A. (1999). A critical evaluation of the mechanisms of action proposed for the antitumor effects of the anthracycline antibiotics adriamycin and daunorubicin. *Biochem. Pharmacol.* **57**, 727-741.

Giunta, S., Belotserkovskaya, R. and Jackson, S. P. (2010). DNA damage signaling in response to double-strand breaks during mitosis. *J. Cell Biol.* **190**, 197-207.

Green, P. S. and Leeuwenburgh, C. (2002). Mitochondrial dysfunction is an early indicator of doxorubicin-induced apoptosis. *Biochim. Biophys. Acta* **1588**, 94-101.

Ha, G. H., Kim, H. S., Lee, C. G., Park, H. Y., Kim, E. J., Shin, H. J., Lee, J. C., Lee, K. W. and Lee, C. W. (2009). Mitotic catastrophe is the predominant response to histone acetyltransferase depletion. *Cell Death Differ.* **16**, 483-497.

Hekmat-Nejad, M., You, Z., Yee, M. C., Newport, J. W. and Cimprich, K. A. (2000). Xenopus ATR is a replication-dependent chromatin-binding protein required for the DNA replication checkpoint. *Curr. Biol.* **10**, 1565-1573.

Huang, X., Tran, T., Zhang, L., Hatcher, R. and Zhang, P. (2005). DNA damage-induced mitotic catastrophe is mediated by the Chk1-dependent mitotic exit DNA damage checkpoint. *Proc. Natl. Acad. Sci. USA* **102**, 1065-1070.

Ichijima, Y., Sakasai, R., Okita, N., Asahina, K., Mizutani, S. and Teraoka, H. (2005). Phosphorylation of histone H2AX at M phase in human cells without DNA damage response. *Biochem. Biophys. Res. Commun.* **336**, 807-812.

Kastan, M. B. and Lim, D. S. (2000). The many substrates and functions of ATM. *Nat. Rev. Mol. Cell Biol.* **1**, 179-186.

Kil, W. J., Cerna, D., Burgan, W. E., Beam, K., Carter, D., Steeg, P. S., Tofilon, P. J. and Camphausen, K. (2008). In vitro and in vivo radiosensitization induced by the DNA methylating agent temozolomide. *Clin. Cancer Res.* **14**, 931-938.

Kodym, E., Kodym, R., Choy, H. and Saha, D. (2008). Sustained metaphase arrest in response to ionizing radiation in a non-small cell lung cancer cell line. *Radiat. Res.* **169**, 46-58.

Loffler, H., Lukas, J., Bartek, J. and Kramer, A. (2006). Structure meets function-centrosomes, genome maintenance and the DNA damage response. *Exp. Cell Res.* **312**, 2633-2640.

Momparler, R. L., Karon, M., Siegel, S. E. and Avila, F. (1976). Effect of adriamycin on DNA, RNA, and protein synthesis in cell-free systems and intact cells. *Cancer Res.* **36**, 2891-2895.

Nabha, S. M., Mohammad, R. M., Dandashi, M. H., Coupaye-Gerard, B., Aboukameel, A., Pettit, G. R. and Al-Katib, A. M. (2002). Combretastatin-A4 prodrug induces mitotic catastrophe in chronic lymphocytic leukemia cell line independent of caspase activation and poly(ADP-ribose) polymerase cleavage. *Clin. Cancer Res.* **8**, 2735-2741.

Niida, H., Tsuge, S., Katsuno, Y., Konishi, A., Takeda, N. and Nakanishi, M. (2005). Depletion of Chk1 leads to premature activation of Cdc2-cyclin B and mitotic catastrophe. *J. Biol. Chem.* **280**, 39246-39252.

Niikura, Y., Dixit, A., Scott, R., Perkins, G. and Kitagawa, K. (2007). BUB1 mediation of caspase-independent mitotic death determines cell fate. *J. Cell Biol.* **178**, 283-296.

Olsson, M., Vakifahmetoglu, H., Abruzzo, P. M., Hogstrand, K., Grandien, A. and Zhivotovsky, B. (2009). DISC-mediated activation of caspase-2 in DNA damage-induced apoptosis. *Oncogene* **28**, 1949-1959.

Park, S. S., Eom, Y. W. and Choi, K. S. (2005). Cdc2 and Cdk2 play critical roles in low dose doxorubicin-induced cell death through mitotic catastrophe but not in high dose doxorubicin-induced apoptosis. *Biochem. Biophys. Res. Commun.* **334**, 1014-1021.

Park, S. S., Kim, M. A., Eom, Y. W. and Choi, K. S. (2007). Bcl-xL blocks high dose doxorubicin-induced apoptosis but not low dose doxorubicin-induced cell death through mitotic catastrophe. *Biochem. Biophys. Res. Commun.* **363**, 1044-1049.

Radford, I. R. and Murphy, T. K. (1994). Radiation response of mouse lymphoid and myeloid cell lines. Part III. Different signals can lead to apoptosis and may influence sensitivity to killing by DNA double-strand breakage. *Int. J. Radiat. Biol.* **65**, 229-239.

Roninson, I. B., Broude, E. V. and Chang, B. D. (2001). If not apoptosis, then what? Treatment-induced senescence and mitotic catastrophe in tumor cells. *Drug Resist. Updat.* **4**, 303-313.

Roschke, A. V., Stover, K., Tonon, G., Schaffer, A. A. and Kirsch, I. R. (2002). Stable karyotypes in epithelial cancer cell lines despite high rates of ongoing structural and numerical chromosomal instability. *Neoplasia* **4**, 19-31.

Sasaki, Y. F., Saga, A., Akasaka, M., Yoshida, K., Nishidate, E., Su, Y. Q., Matsusaka, N. and Tsuda, S. (1997). In vivo genotoxicity of ortho-phenylphenol, biphenyl, and thiabendazole detected in multiple mouse organs by the alkaline single cell gel electrophoresis assay. *Mutat. Res.* **395**, 189-198.

Spallarossa, P., Garibaldi, S., Altieri, P., Fabbi, P., Manca, V., Nasti, S., Rossettin, P., Ghigliotti, G., Ballestrero, A., Patrone, F. et al. (2004). Carvedilol prevents doxorubicin-induced free radical release and apoptosis in cardiomyocytes in vitro. *J. Mol. Cell. Cardiol.* **37**, 837-846.

Tinel, A. and Tschopp, J. (2004). The PIDDosome, a protein complex implicated in activation of caspase-2 in response to genotoxic stress. *Science* **304**, 843-846.

Toh, W. H., Nam, S. Y. and Sabapathy, K. (2010). An essential role for p73 in regulating mitotic cell death. *Cell Death Differ.* **17**, 787-800.

Tsang, W. P., Chau, S. P., Kong, S. K., Fung, K. P. and Kwok, T. T. (2003). Reactive oxygen species mediate doxorubicin induced p53-independent apoptosis. *Life Sci.* **73**, 2047-2058.

Vakifahmetoglu, H., Olsson, M., Orrenius, S. and Zhivotovsky, B. (2006). Functional connection between p53 and caspase-2 is essential for apoptosis induced by DNA damage. *Oncogene* **25**, 5683-5692.

Vakifahmetoglu, H., Olsson, M., Tamm, C., Heidari, N., Orrenius, S. and Zhivotovsky, B. (2008). DNA damage induces two distinct modes of cell death in ovarian carcinomas. *Cell Death Differ.* **15**, 555-566.

Vitale, I., Antoccia, A., Crateri, P., Leone, S., Arancia, G. and Tanzarella, C. (2005). Caspase-independent apoptosis is activated by diazepam-induced mitotic failure in HeLa cells, but not in human primary fibroblasts. *Apoptosis* **10**, 909-920.

Waldman, T., Lengauer, C., Kinzler, K. W. and Vogelstein, B. (1996). Uncoupling of S phase and mitosis induced by anticancer agents in cells lacking p21. *Nature* **381**, 713-716.

Wang, G. W., Klein, J. B. and Kang, Y. J. (2001). Metallothionein inhibits doxorubicin-induced mitochondrial cytochrome c release and caspase-3 activation in cardiomyocytes. *J. Pharmacol. Exp. Ther.* **298**, 461-468.

Woods, C. M., Zhu, J., McQueney, P. A., Bollag, D. and Lazarides, E. (1995). Taxol-induced mitotic block triggers rapid onset of a p53-independent apoptotic pathway. *Mol. Med.* **1**, 506-526.

Yu, C. K. (1964). Chromosomes of X-ray-induced giant cells in chinese hamster in vitro. *Nature* **204**, 1334-1335.

A

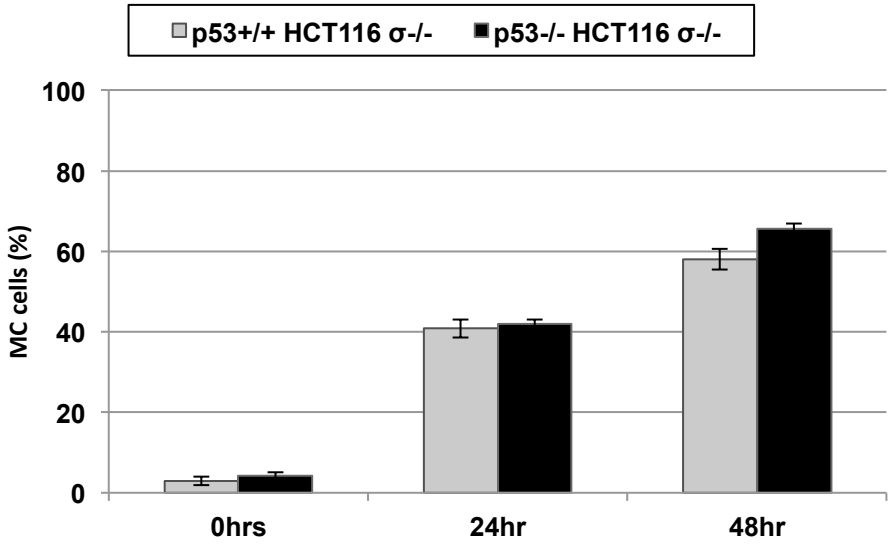

Quantification of MC cells in 14-3-3σ knockout HCT116 and 14-3-3σ and p53 double knockout HCT116 cells untreated or treated with 600 nM doxorubicin. Error bars represent the mean of three independent experiments ± s.e.m.

B

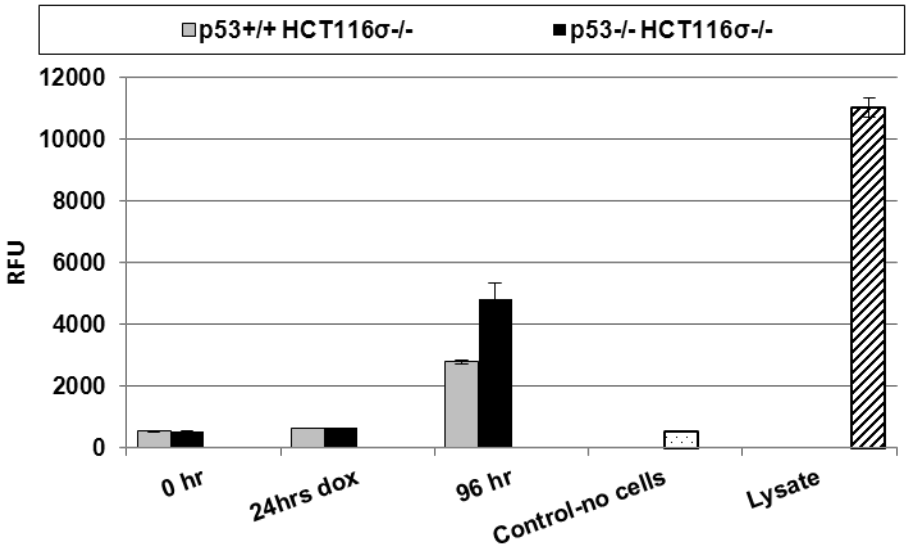

LDH release in $p53^{+/+}$HCT116 and $p53^{-/-}$ HCT116 cells treated with 600 nM doxorubicin for 24 and 96 hours. As positive control the supernatant from lysed cells was used. Error bars represent the mean of three independent experiments ± s.e.m.

C

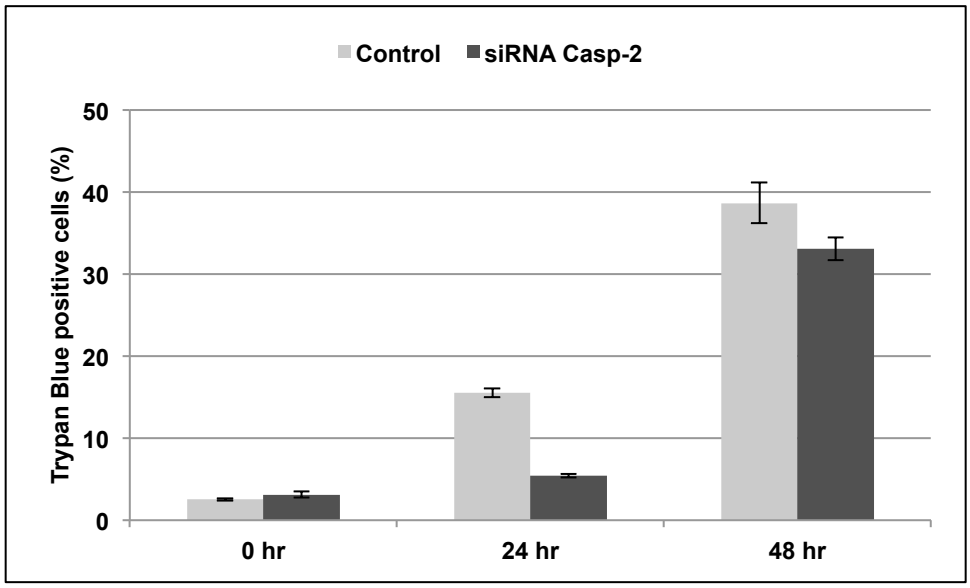

Quantification of cell death in 14-3-3σ$^{-/-}$ HCT116 and 14-3-3σ$^{-/-}$ HCT116 caspase 2$^{-/-}$ cells, untreated or treated with 600 nM doxorubicin using trypan blue staining . Error bars represent the mean of three independent experiments ± s.e.m.

D

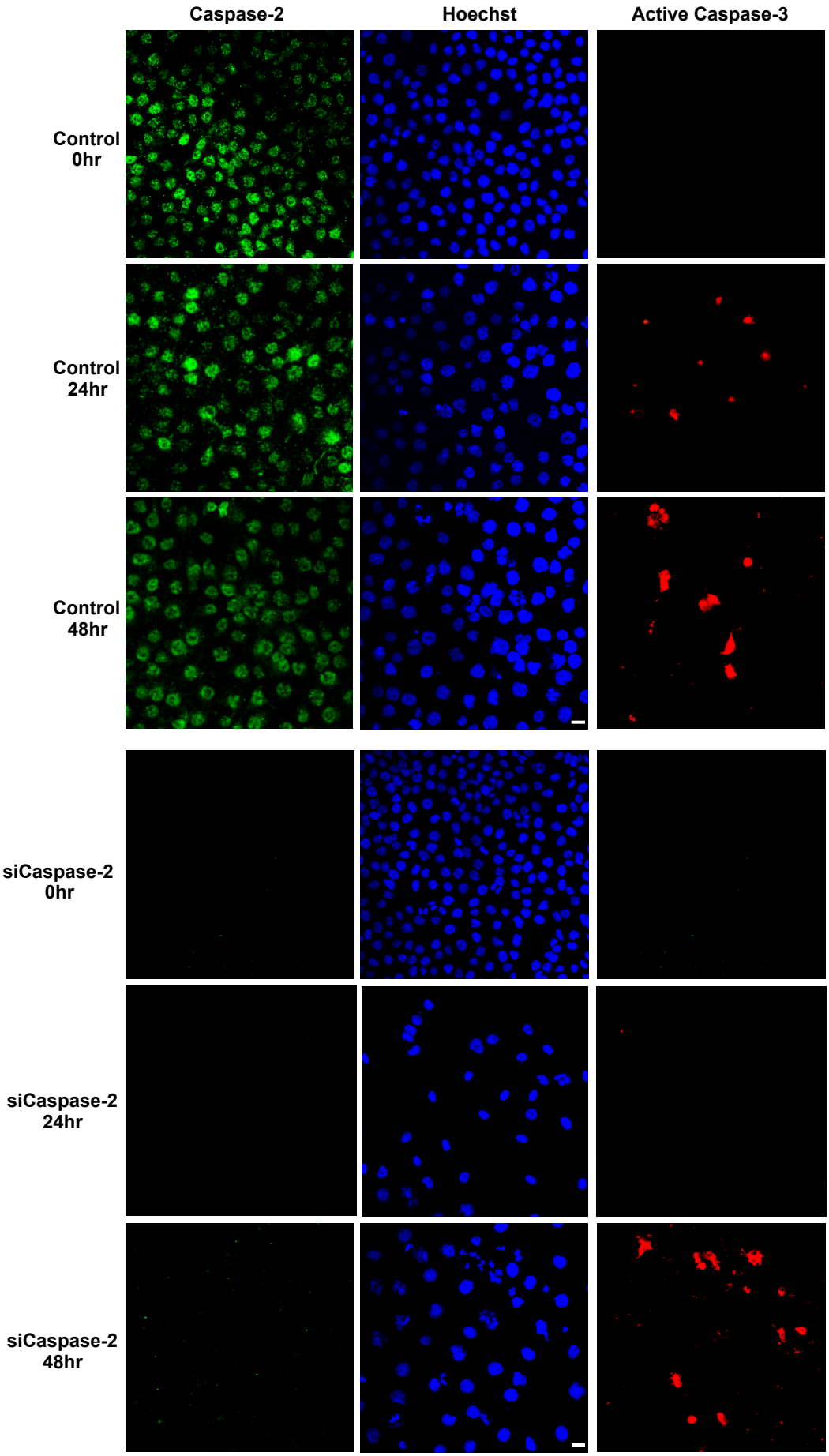
Caspase-2
Hoechst
Active Caspase-3
Control 0hr
Control 24hr
Control 48hr
siCaspase-2 0hr
siCaspase-2 24hr
siCaspase-2 48hr

A

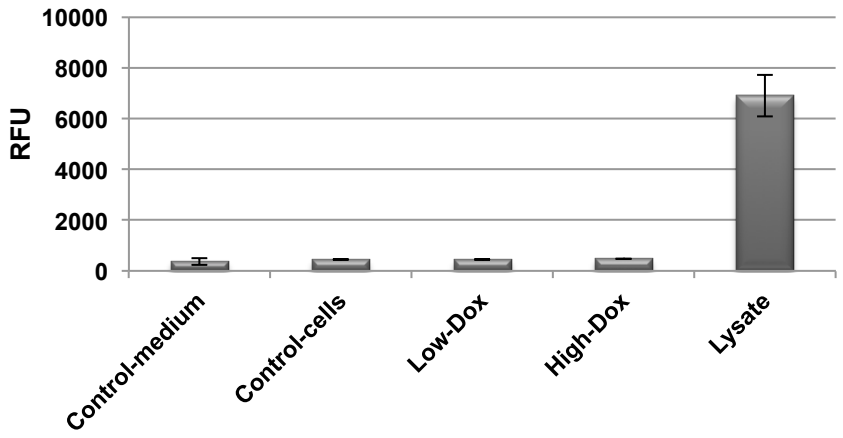

LDH release in 14-3-3σ$^{-/-}$ HCT116 cells treated with low (600 nM) and high (2 μM) doses doxorubicin for 24 hrs. As positive control the supernatant from lysed cells was used. Error bars represent the mean of three independent experiments ± s.e.m.

B

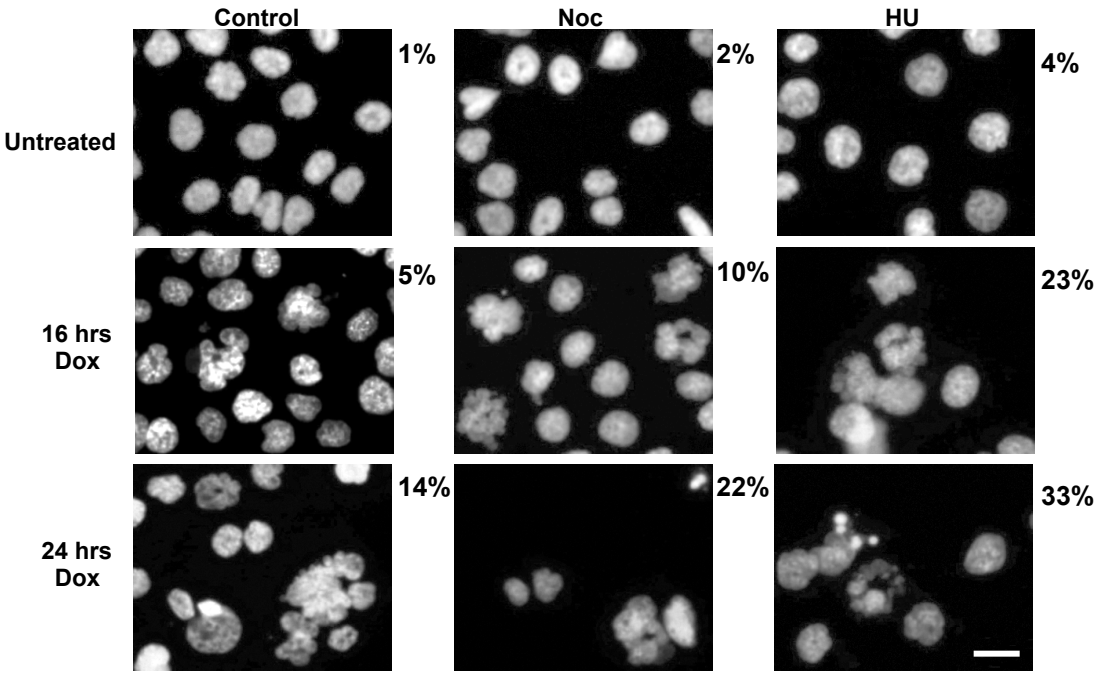

Representative images of M-phase or G1-S-phase synchronised 14-3-3σ$^{-/-}$ HCT116 cells in control and after doxorubicin (600 nM) treatment. Quantification of apoptotic cells corresponding to each treatment is shown beside each image. Bars 20 μM

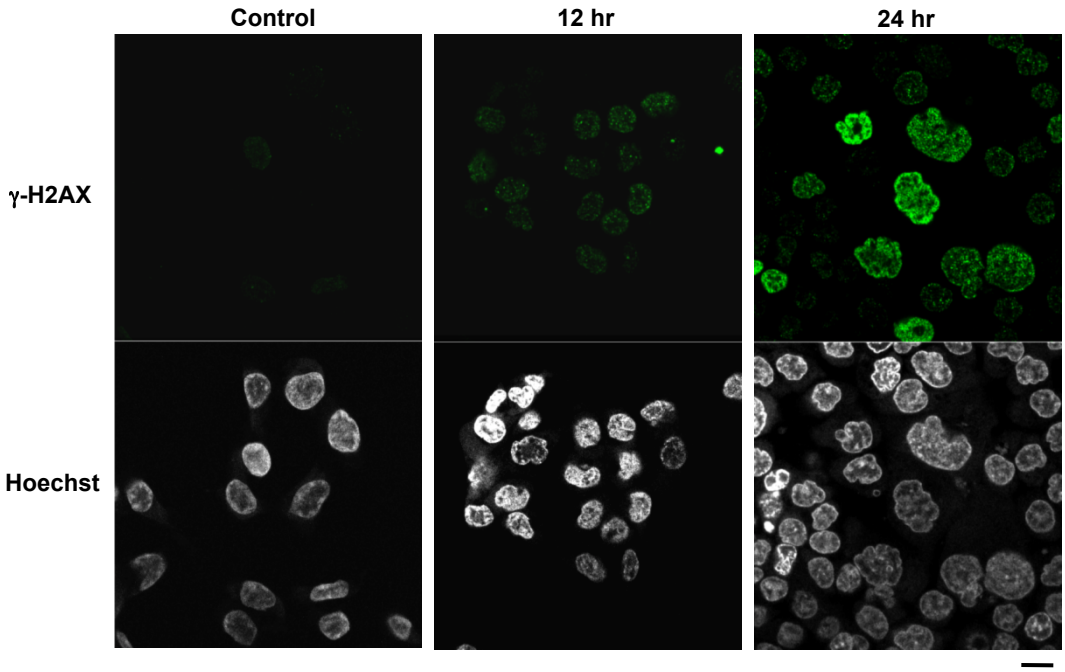

Representative confocal images of untreated and treated p53 -/- cells with 5-fluorouracil (375 μM) for 12 and 24 hours. Staining with antibodies against γ-H2AX and with Hoechst. Bar 20 μM.